AD-A079 806 MCDONNELL DOUGLAS RESEARCH LABS ST LOUIS MO F/G 11/6
INFLUENCE OF RARE-EARTH ADDITIONS ON PROPERTIES OF TITANIUM ALL--ETC(U)
MAY 79 S M SASTRY, R J LEDERICH, P S PAO N00014-76-C-0626
UNCLASSIFIED MDC-Q0684 NL

| OF |
ADA
079806

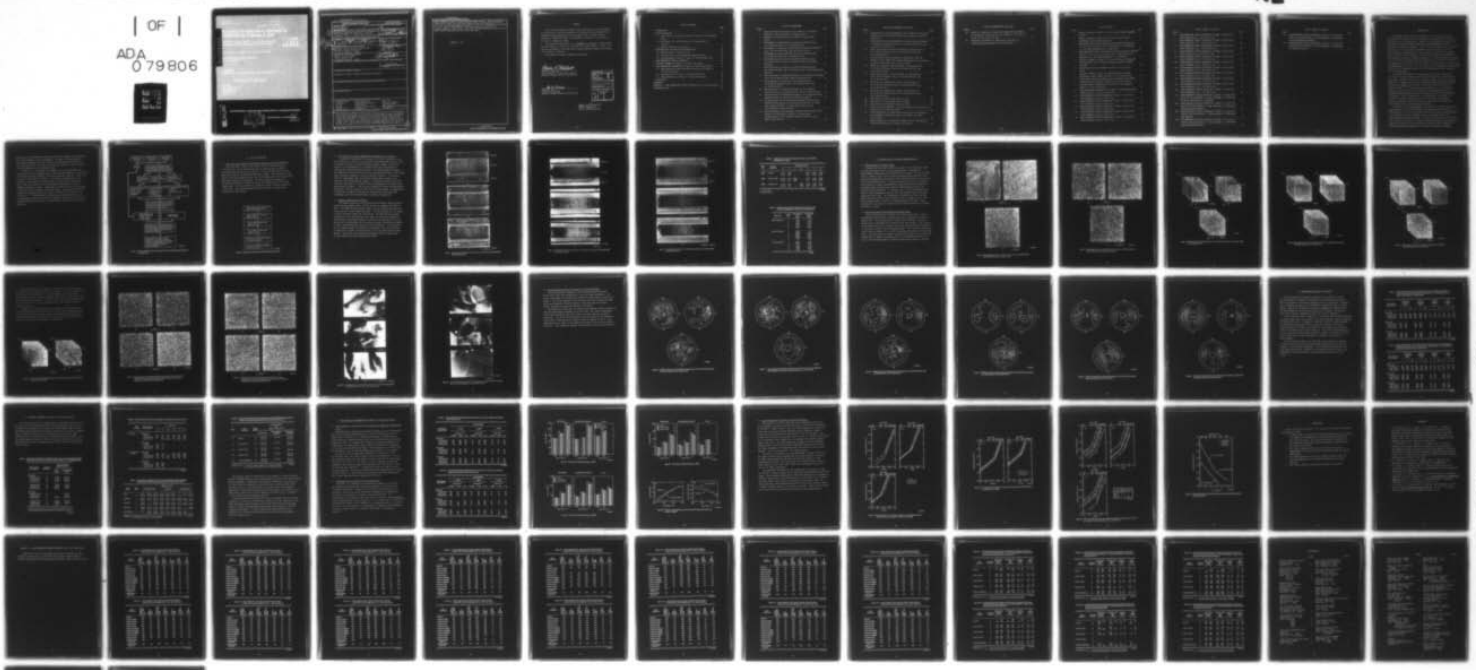

END
DATE
FILMED
2-80
DDC

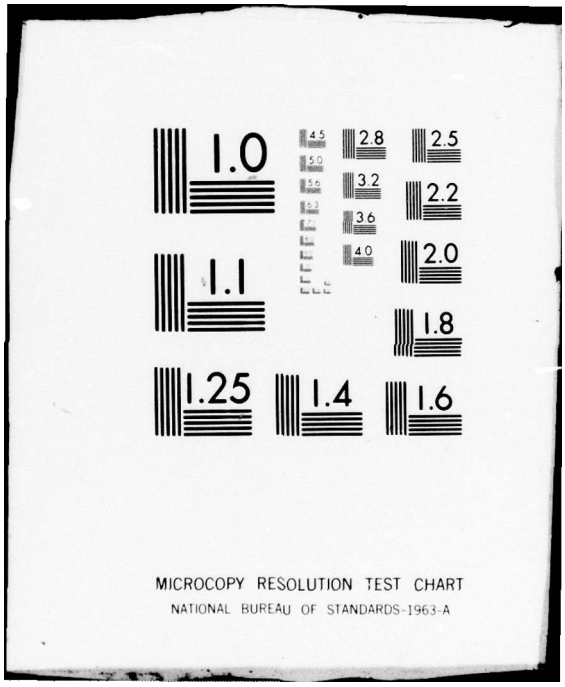
1.0
1.1
1.25
1.4
1.6
1.8
2.0
2.2
2.5
2.8
3.2
3.6
4.0
4.5
5.0
5.6
6.3
MICROCOPY RESOLUTION TEST CHART
NATIONAL BUREAU OF STANDARDS-1963-A

MCDONNELL DOUGLAS RESEARCH LABORATORIES

MCDONNELL DOUGLAS CORPORATION

UNCLASSIFIED

SECURITY CLASSIFICATION OF THIS PAGE (When Data Entered)

REPORT DOCUMENTATION PAGE

READ INSTRUCTIONS BEFORE COMPLETING FORM

1. REPORT NUMBER (14) MDC-Q0684

2. GOVT ACCESSION NO.

3. RECIPIENT'S CATALOG NUMBER (9)

4. TITLE (and Subtitle) (6)
INFLUENCE OF RARE-EARTH ADDITIONS ON PROPERTIES OF TITANIUM ALLOYS. Plane-Strain Fracture Toughness, Creep, and High-Temperature Deformation of Ti-6Al-4V with Erbium and Yttrium Additions.

5. TYPE OF REPORT & PERIOD COVERED
Technical Report, 1 Apr [redacted]78-31 Mar [redacted]79

6. PERFORMING ORG. REPORT NUMBER

7. AUTHOR(s) (10) Shankar James
M. L. Sastry, Richard J. Lederich, Peter S. Pao, and E. O'Neal

8. CONTRACT OR GRANT NUMBER(s) (15)
N0014-76-C-0626

9. PERFORMING ORGANIZATION NAME AND ADDRESS
McDonnell Douglas Research Laboratories
McDonnell Douglas Corporation
St. Louis, Missouri 63166

10. PROGRAM ELEMENT, PROJECT, TASK AREA & WORK UNIT NUMBERS
(12) 70

11. CONTROLLING OFFICE NAME AND ADDRESS
Office of Naval Research
800 N. Quincy Street
Arlington, Virginia 22217

12. REPORT DATE (11)
31 May [redacted]79

13. NUMBER OF PAGES
69

14. MONITORING AGENCY NAME & ADDRESS (if different from Controlling Office)

15. SECURITY CLASS. (of this report)
Unclassified

15a. DECLASSIFICATION/DOWNGRADING SCHEDULE

16. DISTRIBUTION STATEMENT (of this Report)
Approved for public release; distribution unlimited.

17. DISTRIBUTION STATEMENT (of the abstract entered in Block 20, if different from Report)

18. SUPPLEMENTARY NOTES

19. KEY WORDS (Continue on reverse side if necessary and identify by block number)

Titanium alloy	Grain refinement	Ductility
Ti-6Al-4V	Second-phase dispersion	Fracture toughness
Yttrium	Yield stress	Superplasticity
Erbium	Ultimate tensile stress	High temperature deformation
Microstructure	Elongation	Forgeability

20. ABSTRACT (Continue on reverse side if necessary and identify by block number)
The influence of additions of 0.05 wt% Y and 0.1 wt% Er on the room-temperature tensile properties, plane-strain and plane-stress fracture toughness, creep, and high-temperature high-strain-rate deformation characteristics of Ti-6Al-4V was studied. 75 kg ingots of Ti-6Al-4V, Ti-6Al-4V-0.05Y and Ti-6Al-4V-0.1Er were cast, forged, and rolled into 80-mm, 30-mm, and 13-mm plates. The Y and Er additions reduce the high-temperature flow stress of Ti-6Al-4V at strain rates of 0.05 and 0.5/s and significantly improve →
next page

DD FORM 1 JAN 73 1473 EDITION OF 1 NOV 65 IS OBSOLETE

405 315

UNCLASSIFIED

SECURITY CLASSIFICATION OF THIS PAGE (When Data Entered)

ingot-breakdown forging by suppressing the edge cracking. The Y-containing Ti-6Al-4V has lower flow stress and higher strain-rate sensitivity of flow stress and consequently better superplasticity than the reference alloy at 906°C at strain rates of 10^{-5}-10^{-3} s^{-1}. The room-temperature plane-strain fracture toughness, yield stress, ductility, and high-temperature creep are not significantly altered by the rare-earth additions.

.00001 to .001

PREFACE

This report presents the results of the third phase of an investigation of the effects of rare-earth additives on titanium alloys performed by the McDonnell Douglas Research Laboratories under Office of Naval Research contract No. N00014-76-C-0626. The scientific officer for the contract is Dr. Bruce A. MacDonald of ONR.

The principal investigator is Dr. Shankar M. L. Sastry; co-investigators are Mr. Richard J. Lederich, Dr. Peter S. Pao, and Mr. James E. O'Neal. The work was performed in the Solid State Sciences department under the direction of Dr. Charles R. Whitsett.

This report has been reviewed and is approved.

Charles R. Whitsett

Charles R. Whitsett
Chief Scientist - Solid State Sciences
McDonnell Douglas Research Laboratories

D. P. Ames

Donald P. Ames
Staff Vice President
McDonnell Douglas Research Laboratories

Bruce A MacDonald

Bruce A. MacDonald
Office of Naval Research

TABLE OF CONTENTS

LIST OF ILLUSTRATIONS

LIST OF ILLUSTRATIONS (continued)

LIST OF ILLUSTRATIONS (continued)

LIST OF TABLES

LIST OF TABLES (continued)

LIST OF TABLES (continued)

1. INTRODUCTION

A systematic investigation was conducted of the effects of metallic rare-earth (RE) additions on the microstructure and properties of Ti-6Al-4V. The objective of the program was to improve the high-temperature formability of Ti-6Al-4V without adversely affecting the room-temperature tensile properties and fracture toughness. In the first two phases of this contract[1,2], the effects of yttrium, erbium, mischmetal, and yttria additions on the microstructure, room-temperature tensile properties, and fracture toughness (K_Q) of Ti-6Al-4V were determined. In Phase III, research was completed on the influence of metallic rare-earth additions on the microstructure and properties of Ti-6Al-4V by demonstrating that additions of 0.1 wt% Er or 0.05 wt% Y (1) improve the yield during initial forging of Ti-6Al-4V ingots, (2) reduce the high-temperature flow stress, (3) control grain size at β-processing temperatures, and (4) have no significant effect on yield strength and fracture toughness of α-β processed alloy.

A previous study[3] showed that Y_2O_3-additive is a beta-grain refiner in Ti-6Al-4V and significantly improves ingot forgeability. However, when Y_2O_3 powder is added to Ti-6Al-4V, it remains as large (1-10 μm) inclusions, which tend to agglomerate in Ti-6Al-4V and can degrade the tensile strength and fracture toughness, particularly in the short transverse direction. Previous studies[4-6] of metallic rare-earth additives to α-Ti showed that metallic Y and Er dissolve in the molten Ti and precipitate as fine and uniformly dispersed particles, which effectively refine the microstructure of titanium. In this investigation, the approach was to introduce into Ti-6Al-4V a uniform dispersion of fine (< 70 nm diam), second-phase, rare-earth particles, which are particularly effective for refining the alloy microstructure and retarding grain growth.

In Phase I of this investigation, 5-kg ingots of Ti-6Al-4V with various concentrations of Y, Er, and mischmetal were prepared and characterized. Concentrations of 0.1 wt% Er and 0.02-0.05 wt% Y in Ti-6Al-4V were determined to be effective for grain refinement and to not adversely affect the room-temperature tensile properties. In Phase II, 14-kg ingots of Ti-6Al-4V with 0.1 wt% Er, 0.02 wt% Y, 0.05 wt% Y, and 0.038 wt% Y_2O_3, which were cast, forged, and rolled by the Crucible Materials Research Center (CMRC),and were characterized with respect to the effects of different annealing

procedures on room-temperature tensile and fracture-toughness characteristics and crystallographic texture development. The Phase II alloys exhibited beta-grain refinement by Er and Y but were not significantly different at room temperature from the Ti-6Al-4V control alloy except for those properties directly dependent on prior beta-grain size.

In Phase III of the program, the emphasis was on the determination of plane-strain fracture toughness (K_{IC}), creep, and high-temperature, high-strain-rate deformation characteristics of the RE-containing Ti-6Al-4V. Figure 1 is an outline of the Phase III studies. For Phase III (second year of the contract), 75-kg ingots of Ti-6Al-4V with 0.1 wt% Er and 0.05 wt% Y were cast, forged, and rolled by the Titanium Metals Corporation of America (TIMET) in Henderson, Nevada. These Phase-III ingots were the first prepared of sufficient size to simulate production ingots. The rare-earth additions reduced the high-temperature flow stress of Ti-6Al-4V at strain rates of 0.05 and 0.5 s^{-1} and significantly improved ingot-breakdown forging. The room-temperature plane-strain fracture toughness, yield stress, and ductility and high-temperature creep were not significantly altered by the rare-earth additions.

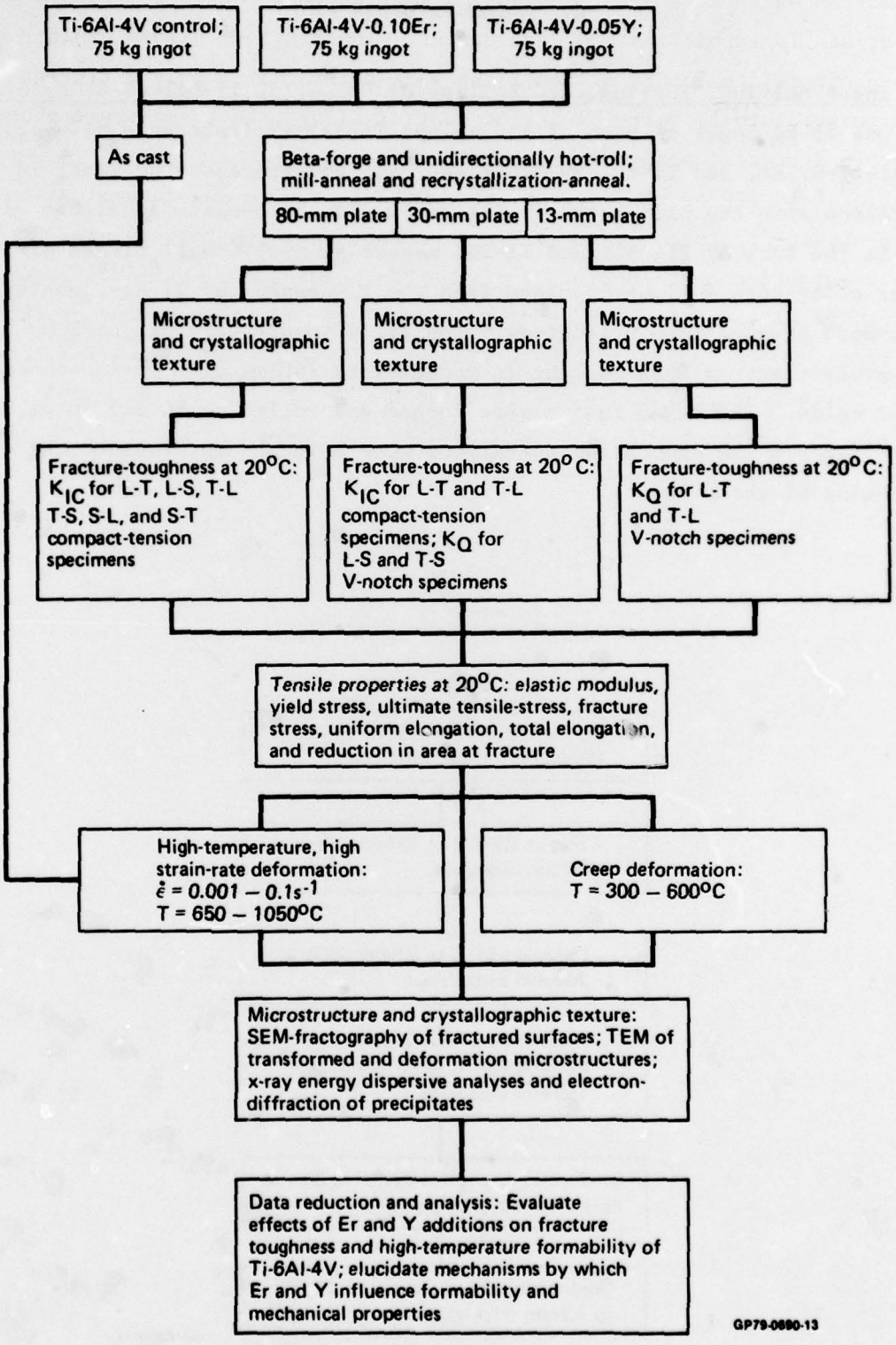

Figure 1. Outline of Phase III research on the effects of rare-earth additions of the properties of titanium alloys.

2. ALLOY PREPARATION

2.1 Ingot Melting, Forging, and Rolling of Phase III Ti-6Al-4V-RE Alloys

One 75-kg ingot of each of the alloys Ti-6Al-4V (reference alloy), Ti-6Al-4V-0.1Er, and Ti-6Al-4V-0.05Y was cast and processed by TIMET in accordance with the plan shown in Figure 2. The rare-earth additions were made in the form of Ti-25Er and Ti-25Y master alloys. Small pieces of Ti-RE master alloy were intimately mixed with the Ti-sponge and Ti-Al-V master alloy, which were pressed into briquettes. The alloy ingots were prepared by consumable-electrode arc melting in vacuum into 160-mm diam, water-cooled, copper molds. The alloy ingots were forged and rolled to 80-mm, 30-mm, and 13-mm plates. The processing operations were selected to simulate the processing of large ingots.

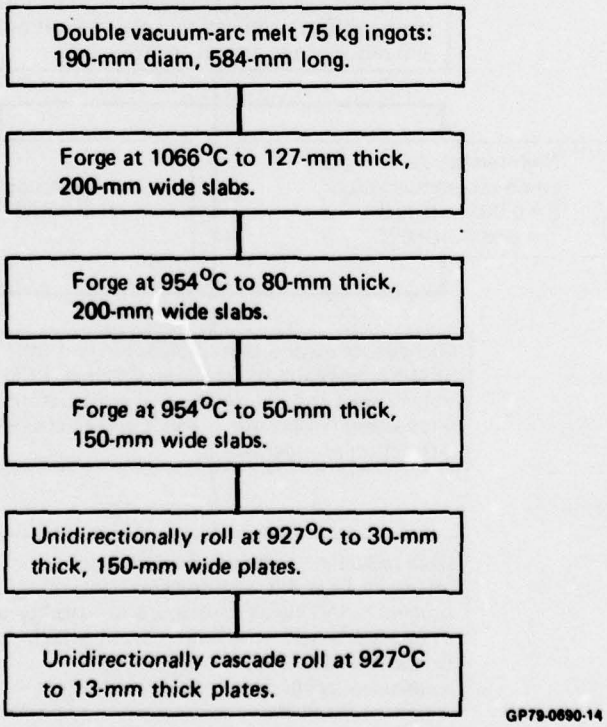

Figure 2. Forging and rolling schedule for Phase III Ti-6Al-4V-RE alloys.

2.2 The Effects of Y and Er Additions on Forgeability of Ti-6Al-4V

A qualitative indication of the effects of Y and Er additions on the hot formability of Ti-6Al-4V was obtained by determining the extent of edge and surface cracking of Ti-6Al-4V during different stages of reduction. Figures 3-5 are photographs of the 80-mm, 30-mm, and 13-mm plates of Ti-6Al-4V-RE alloys processed according to the schedule shown in Figure 2. The significant beneficial effects of the rare-earth additions on the initial ingot break-down forging are clearly revealed in Figure 3. In contrast with the considerable edge- and surface-cracking that occurred on the reference alloy during initial forging, no cracking occurred on the alloys with 0.1Er and 0.05Y as is evident from the photographs of the 80-mm thick plates shown in Figure 3. The rare-earth additions effected an approximately 25% greater yield of crack-free alloy after initial forging. No significant differences in formability between the reference alloy and rare-earth containing alloys were observed after the initial forging step.

2.3 Chemical Analyses of the Alloys

The chemical analyses of the alloys were performed by TIMET and United States Testing Company (USTC), and the results are summarized in Tables 1 and 2. The TIMET analyses shown in Table 1 are for samples taken from the top and bottom of each 160-mm diam ingot. The USTC analyses are for samples cut from the 80-mm, 30-mm, and 13-mm plates. The USTC analytical method consisted of first converting the rare earths to oxalates by dissolving the rare-earth containing specimens in a mixture of hydrofluoric acid and nitric acid, precipitating the rare earths as oxides by heating the samples to 800°C, and analyzing the oxides by x-ray fluorescence. The Y analyses by both companies show lower than the aim chemistry, and this discrepancy is attributed by TIMET to volatilization of the rare earths during vacuum melting. The erbium concentrations determined by USTC are higher than the aim chemistry and those determined by TIMET.

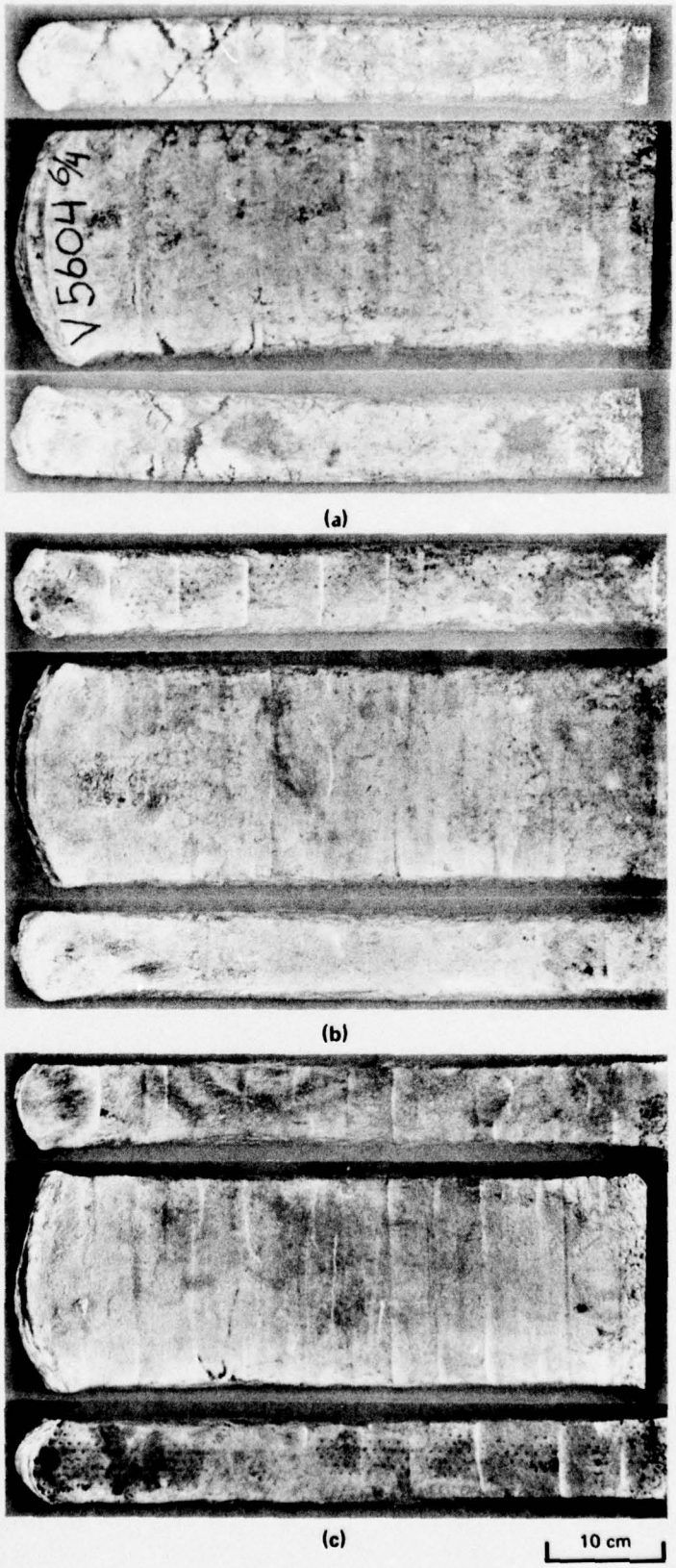

Figure 3. Photographs of forged 80-mm (a) Ti-6Al-4V reference alloy, (b) Ti-6Al-4V-0.05Y, and (c) Ti-6Al-4V-0.1Er

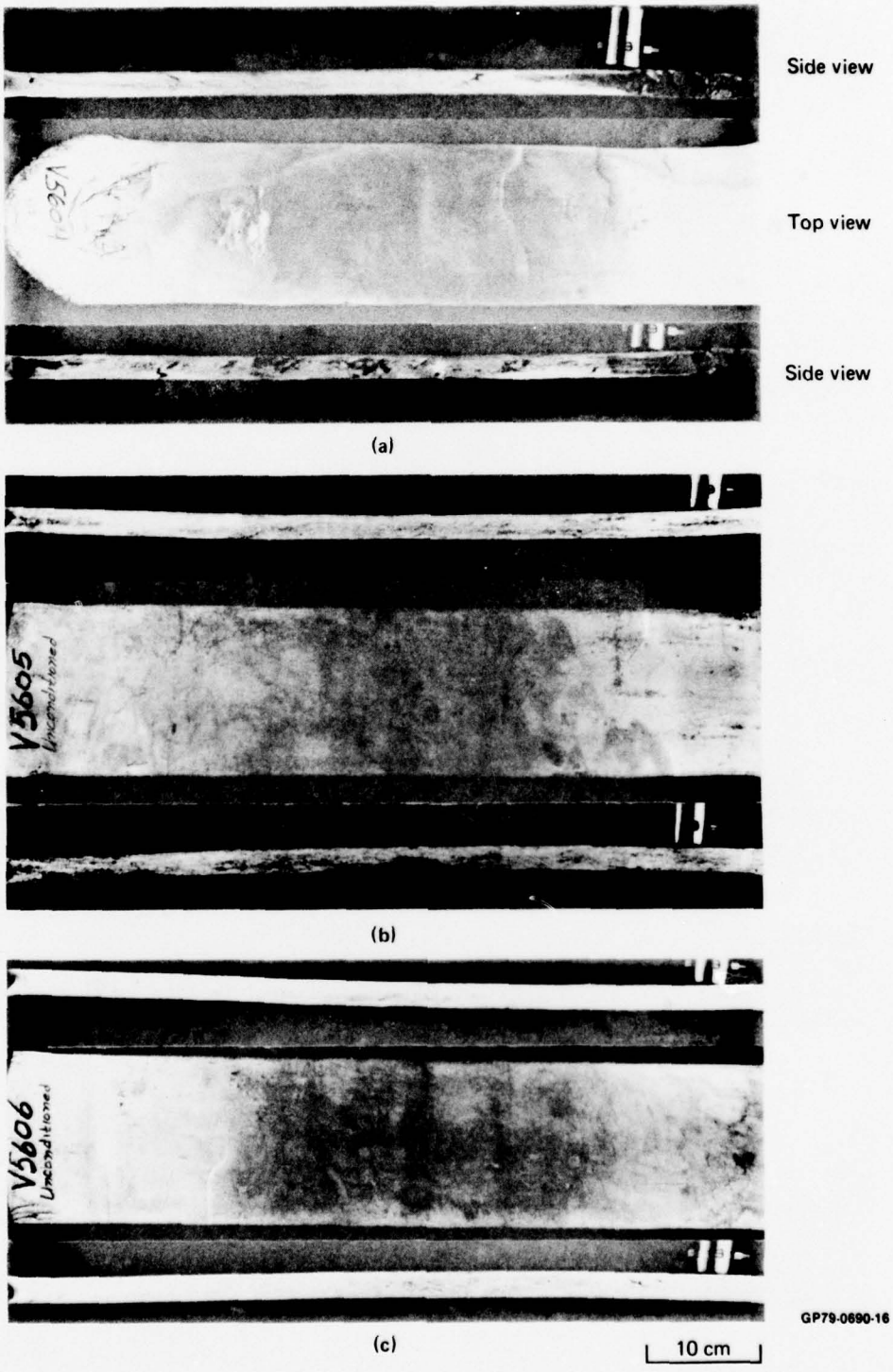

Figure 4. Photographs of forged and rolled 30-mm (a) Ti-6Al-4V reference alloy, (b) Ti-6Al-4V-0.05Y, and (c) Ti-6Al-4V-0.1Er

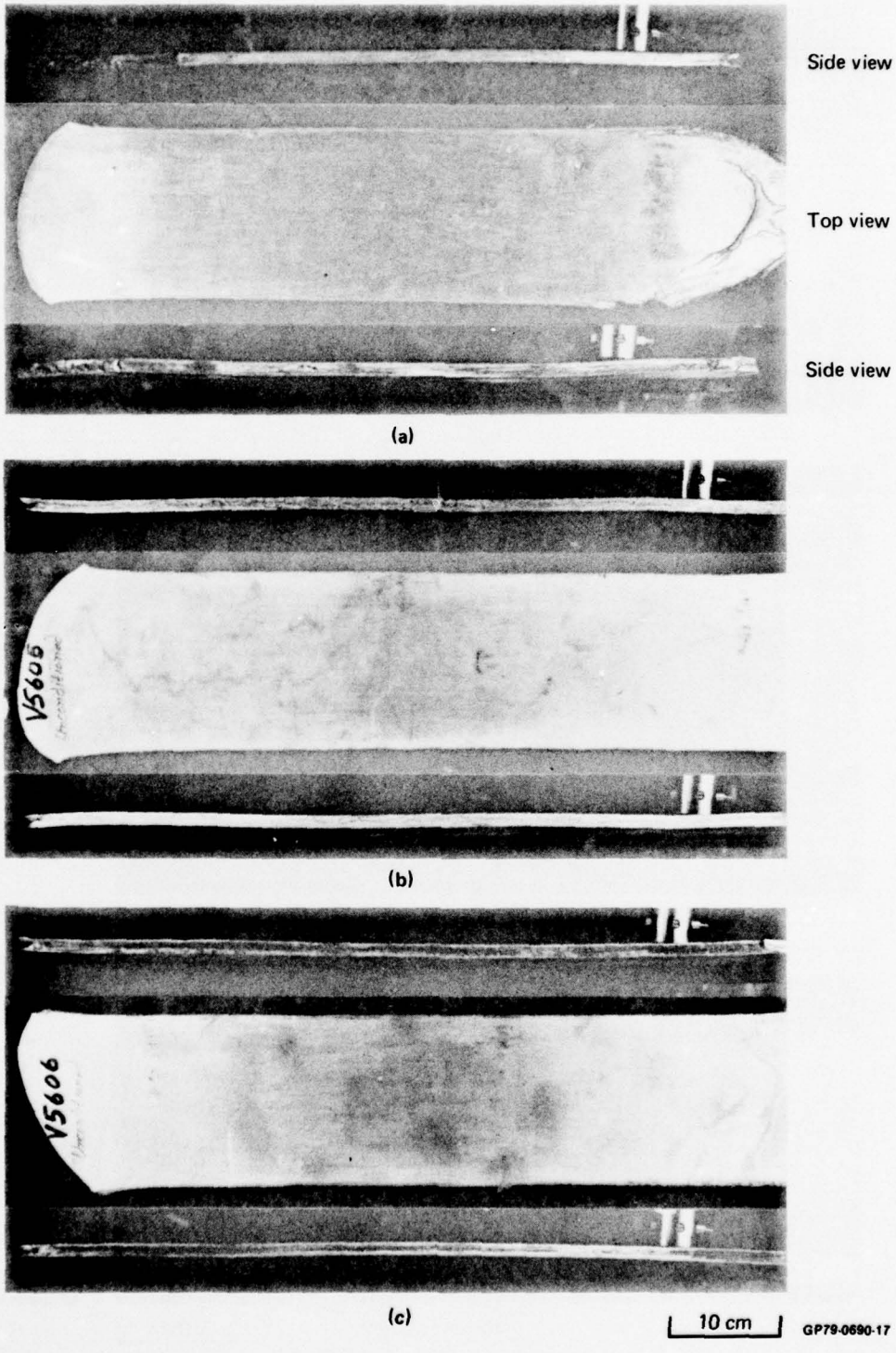

Figure 5. Photographs of rolled 13-mm (a) Ti-6Al-4V reference alloy, (b) Ti-6Al-4V-0.05Y, and (c) Ti-6Al-4V-0.1Er

TABLE 1. CHEMICAL ANALYSES OF PHASE III Ti-6Al-4V ALLOY INGOTS PERFORMED BY TIMET.

Alloy heat no.	Nominal composition		Concentration (wt%)						
			Al	V	Y	Er	N	O	Fe
V5604	Ti-6Al-4V	T	6.14	3.78	–	–	0.016	0.145	0.153
		B	6.16	3.99	–	–	0.017	0.186	0.160
V5605	Ti-6Al-4V-0.05Y	T	6.23	3.97	0.030	–	0.017	0.128	0.169
		B	6.05	4.12	0.030	–	0.017	0.144	0.165
V5606	Ti-6Al-4V-0.1Er	T	6.16	4.04	–	0.061	0.015	0.128	0.154
		B	6.28	4.15	–	0.065	0.016	0.133	0.134

GP79-0880-1

T = Top of the ingot
B = Bottom of the ingot

TABLE 2. CHEMICAL ANALYSES OF PHASE III Ti-6Al-4V-RE ALLOY PLATES PERFORMED BY UNITED STATES TESTING CO.

Alloy plate	Sample no.	Concentration of Y (wt%)	Concentration of Er (wt%)
80-mm thick plate	1	0.008	0.114
	2	0.011	0.178
	3	0.006	0.187
	4	0.013	0.181
	5	0.013	0.132
30-mm thick plate	1	0.025	0.111
	2	<0.005	0.159
	3	<0.005	0.261
	4	<0.005	0.220
	5	0.018	0.090
13-mm thick plate	1	<0.005	0.490
	2	0.017	0.119
	3	0.015	0.136
	4	0.016	0.152
	5	0.008	0.127

GP79-0880-2

3. MICROSTRUCTURE AND TEXTURE CHARACTERIZATION

3.1 Microstructure of As-Cast Alloys

A 25-mm thick slice was cut from the middle of each 75-kg alloy ingot for characterization of the as-cast microstructure. Specimens for metallographic examination were prepared from the centers of the 25-mm thick slices. Figures 6 and 7 show the typical microstructures observed in the radial and perpendicular directions of the Ti-6Al-4V reference alloy and the Y- and Er-containing alloys. The as-cast microstructure of the reference alloy consists of large transformed-beta grains with several colonies of α platelets within each grain and coarse-α formed during cooling at the prior-beta grain boundaries. In contrast, the Y- and Er-containing alloys exhibit a more homogeneous structure with substantially smaller platelet length and colony size. The preferential α-nucleation at the prior-beta grain boundaries observed in the reference alloy is absent in the Y- and Er-containing alloys, in which the α-phase nucleates uniformly. These microstructural features are similar to those observed previously in Phase I and Phase II alloys.

3.2 Microstructures of Hot-Worked and Annealed Alloys

The microstructures of the Phase III reference alloy and Y- and Er-containing alloys processed to 80-mm, 30-mm, and 13-mm plates are shown in Figures 8-10. The microstructure of 80-mm plates consists of acicular, basket weave, transformed beta as expected from beta forging. The acicular-α in the reference alloy is irregular and curved, whereas straight α-platelets are observed in the Er- and Y-containing alloys. The α-platelet lengths and colony sizes are smaller in Y- and Er-containing alloys than in the reference alloy. Upon increasing the amount of working in the alpha + beta field, the microstructure changes to equiaxed alpha in a transformed-beta matrix, as seen in the photomicrographs of 30-mm and 13-mm plates (Figures 9 and 10).

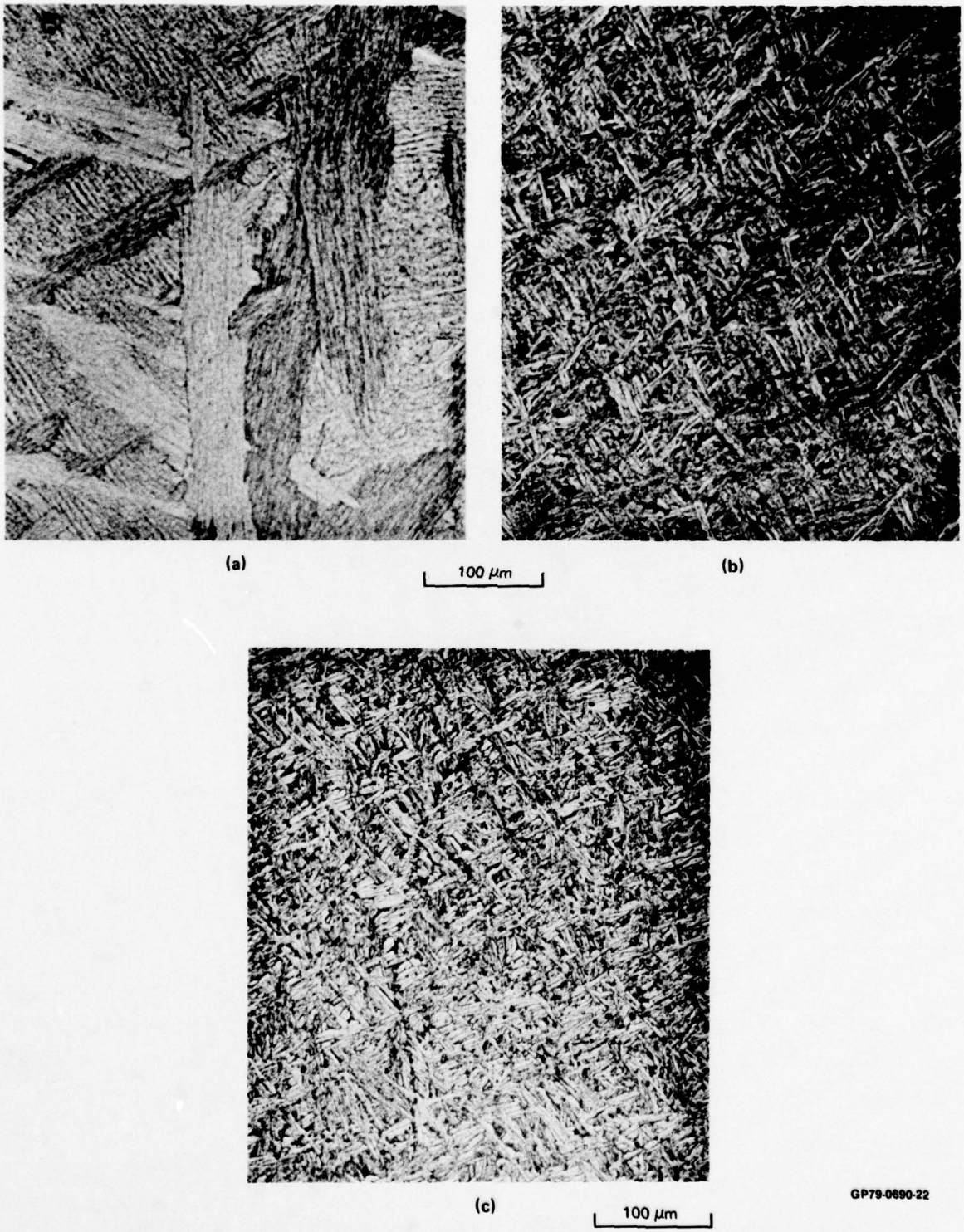

Figure 6. Microstructures of as-cast (a) Ti-6Al-4V reference alloy, (b) Ti-6Al-4V-0.05Y, and (c) Ti-6Al-4V-0.1Er in the radial direction

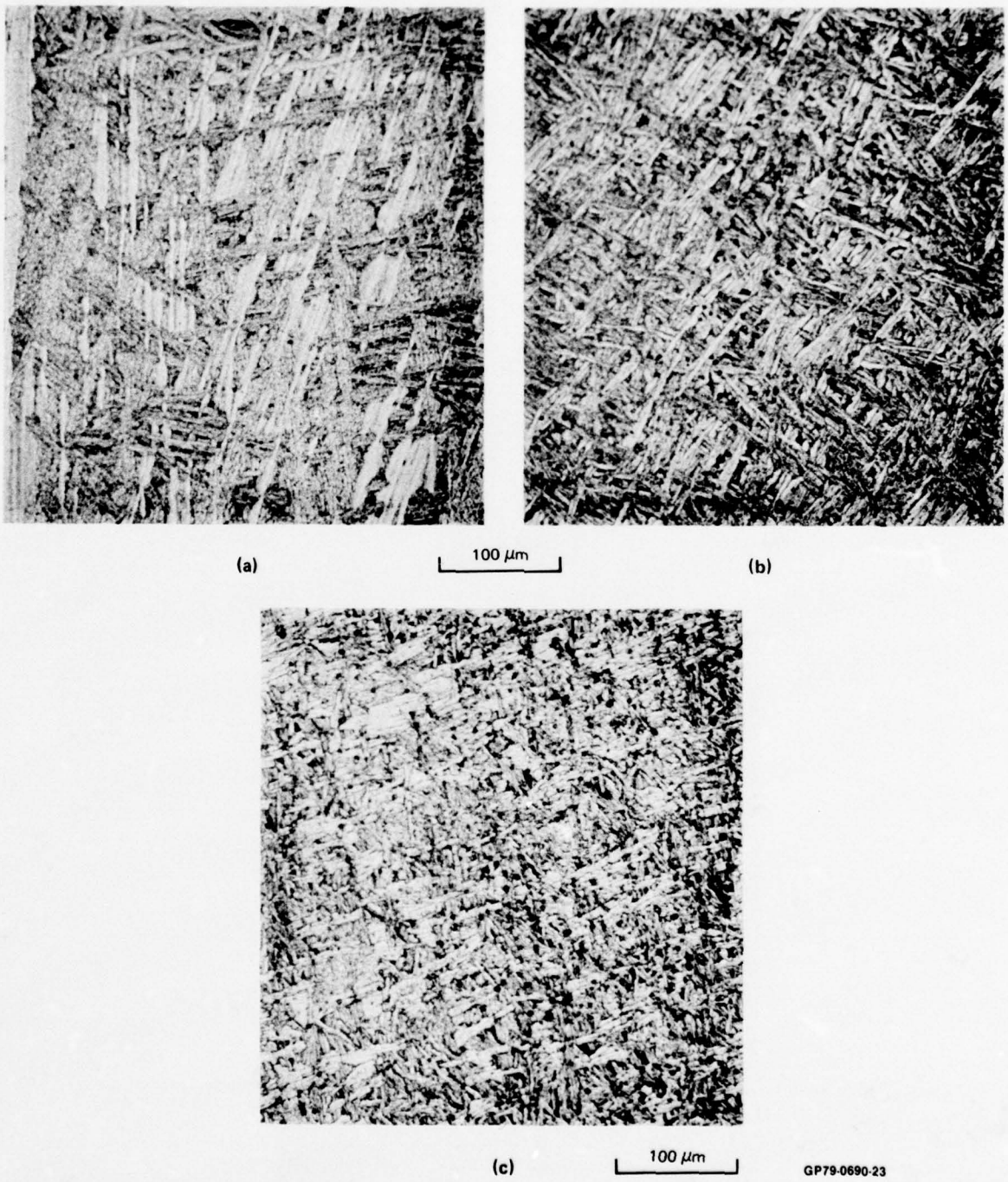

Figure 7. Microstructures of as-cast (a) Ti-6Al-4V reference alloy, (b) Ti-6Al-4V-0.05Y, and (c) Ti-6Al-4V-0.1Er in the perpendicular direction

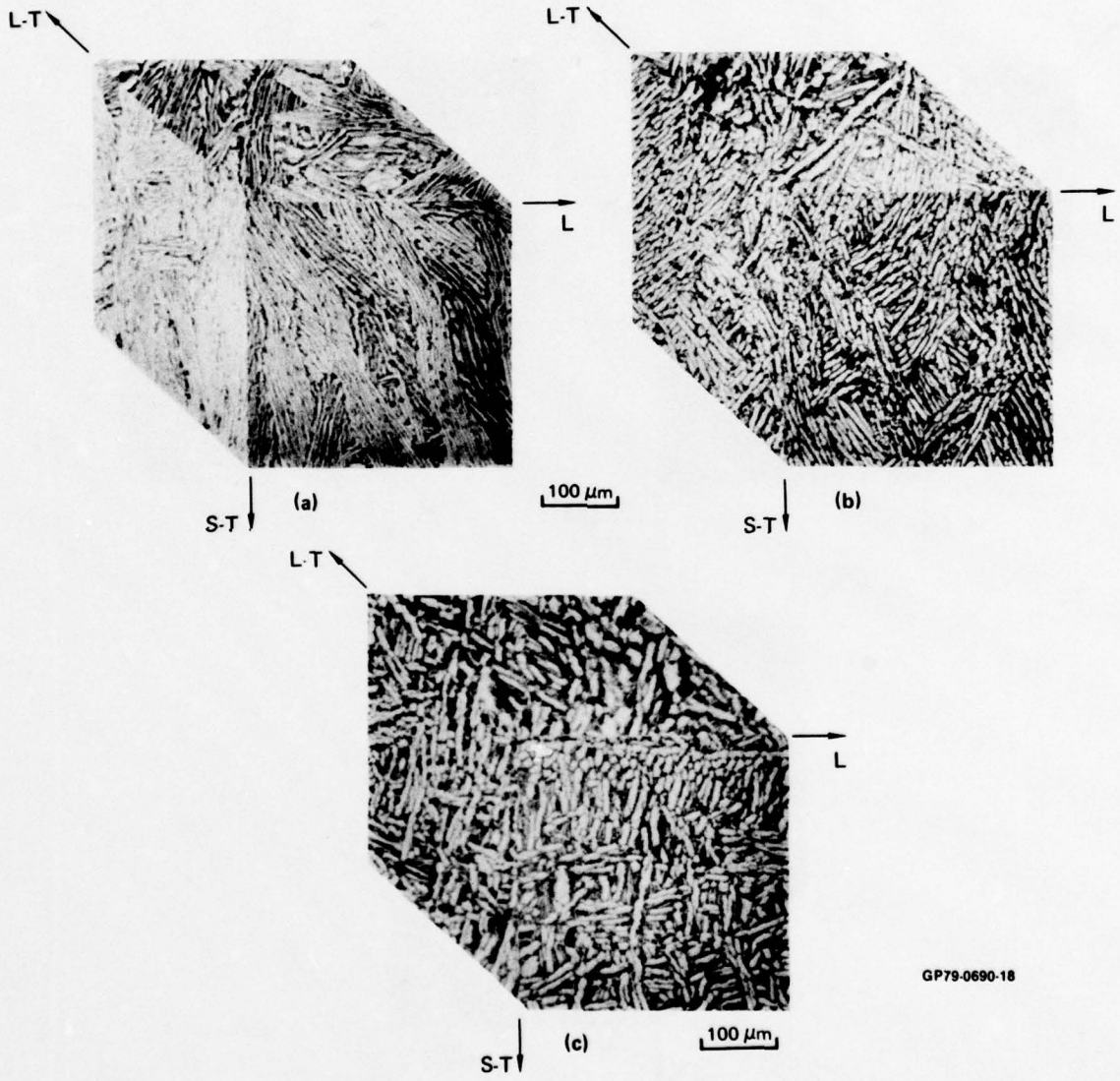

Figure 8. Microstructures of forged 80-mm plates of (a) Ti-6Al-4V reference alloy, (b) Ti-6Al-4V-0.05Y, and (c) Ti-6Al-4V-0.1Er

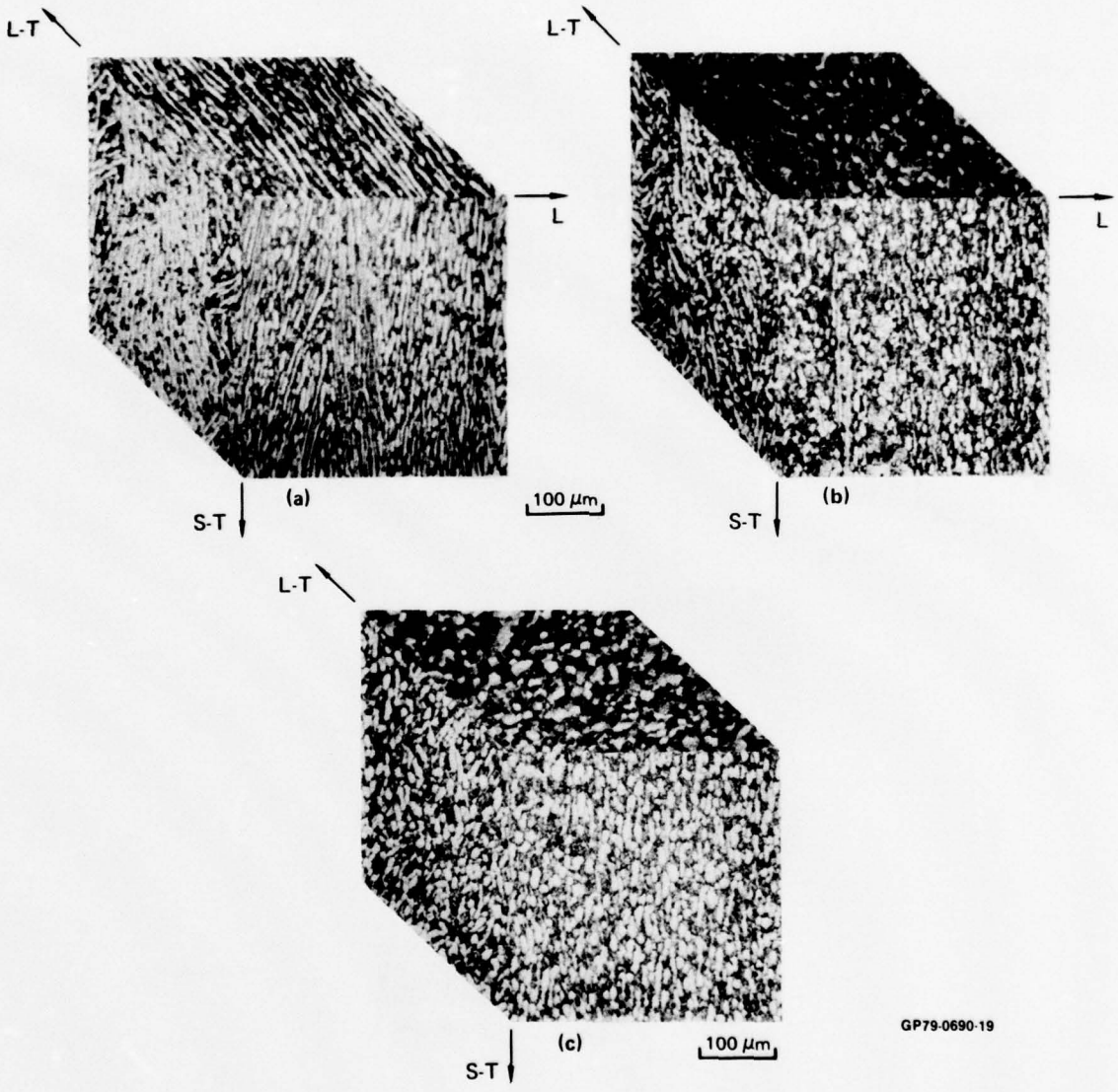

Figure 9. Microstructures of forged and rolled 30-mm plates of (a) Ti-6Al-4V reference alloy, (b) Ti-6Al-4V-0.05Y, and (c) Ti-6Al-4V-0.1Er

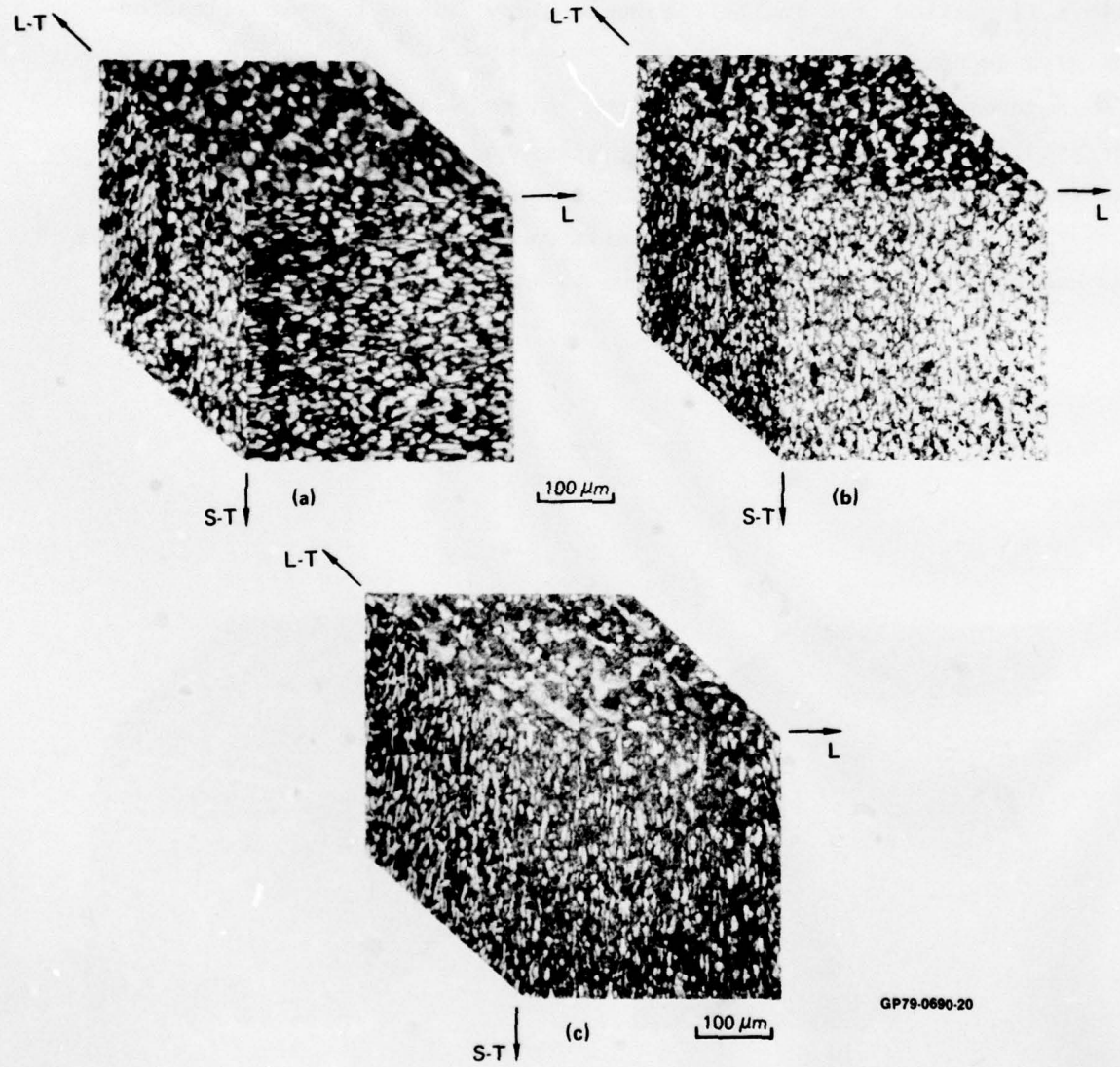

Figure 10. Microstructures of rolled 13-mm plates of (a) Ti-6Al-4V reference alloy, (b) Ti-6Al-4V-0.05Y, and (c) Ti-6Al-4V-0.1Er

The microstructures of the Phase III alloys after recrystallization annealing and mill annealing are shown in Figures 11-13. The recrystallization-annealed 30-mm and 13-mm alloy plates exhibit equiaxed two-phase microstructures, whereas the mill-annealed plates show no significant change in the elongated-α morphology. The grain size in the Y- and Er-containing alloys is smaller than in the reference alloy in the recrystallization-annealed condition.

Figures 14 and 15 are the electron micrographs of mill-annealed and recrystallization-annealed reference alloy and Er- and Y-containing alloys. The rare-earth-containing alloys contain small dispersoids; however, the number of dispersoids in the thin foils was much lower than expected from the nominal rare-earth concentrations in the alloys.

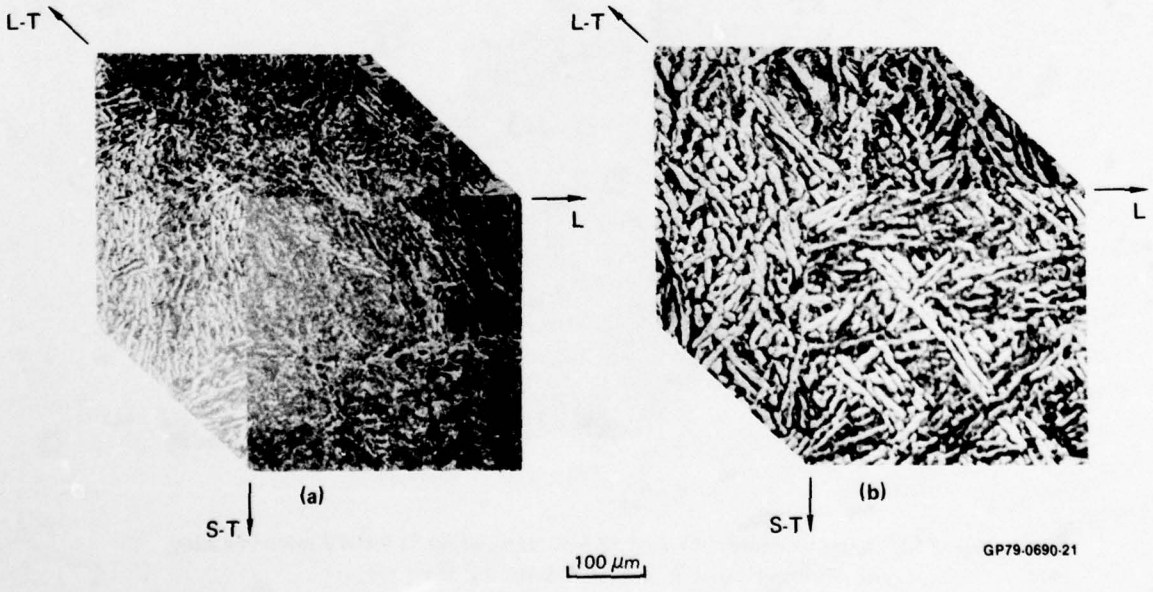

Figure 11. Microstructures of forged 80-mm plates of (a) recrystallization annealed Ti-6Al-4V, and (b) mill annealed Ti-6Al-4V

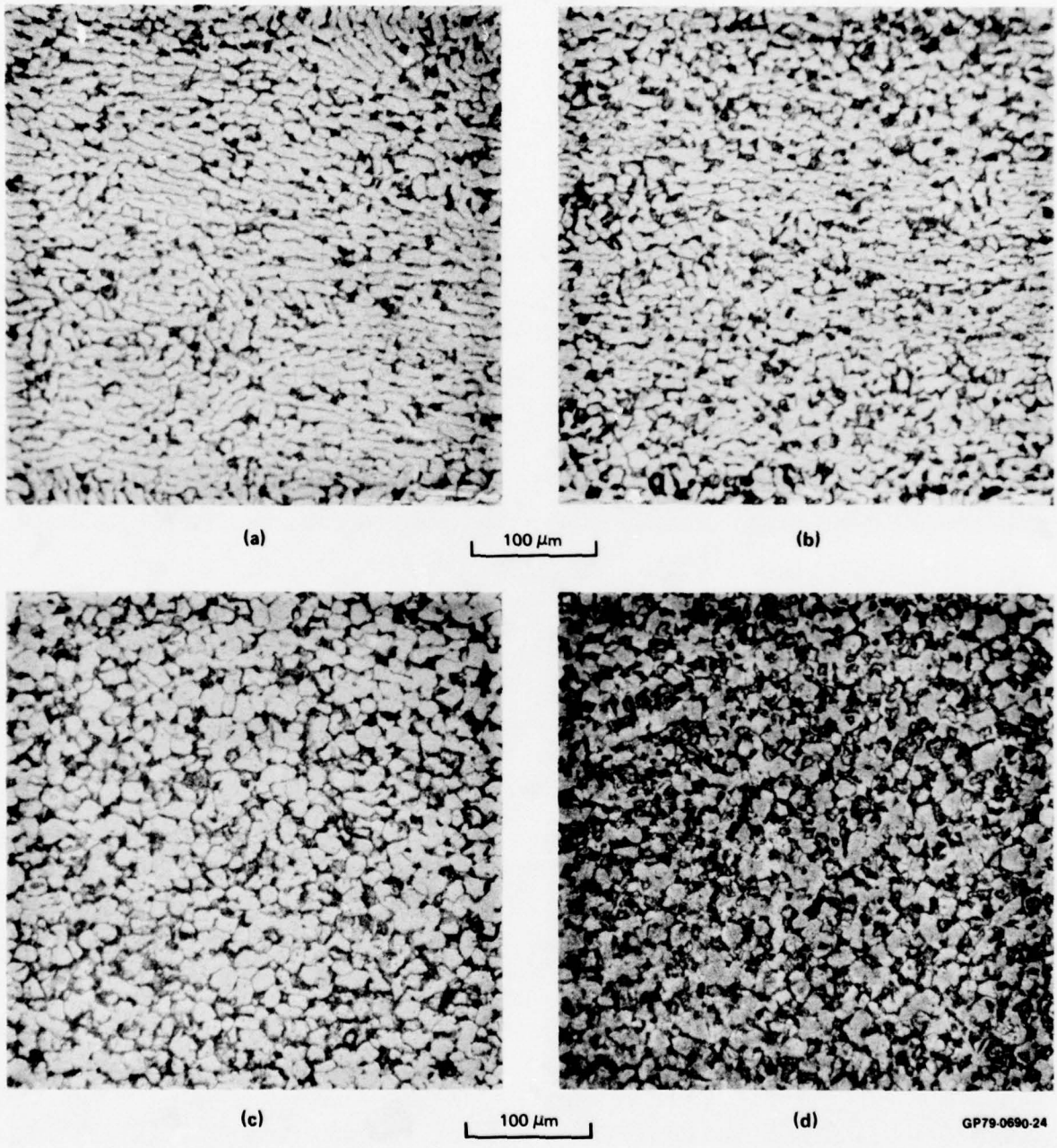

Figure 12. Microstructures of recrystallization annealed *Ti-6Al-4V* and *Ti-6Al-4V-0.05Y* alloys; (a) 30-mm plate Ti-6Al-4V, (b) 30-mm plate Ti-6Al-4V-0.05Y, (c) 13-mm plate Ti-6Al-4V, and (d) 13-mm plate Ti-6Al-4V-0.05Y

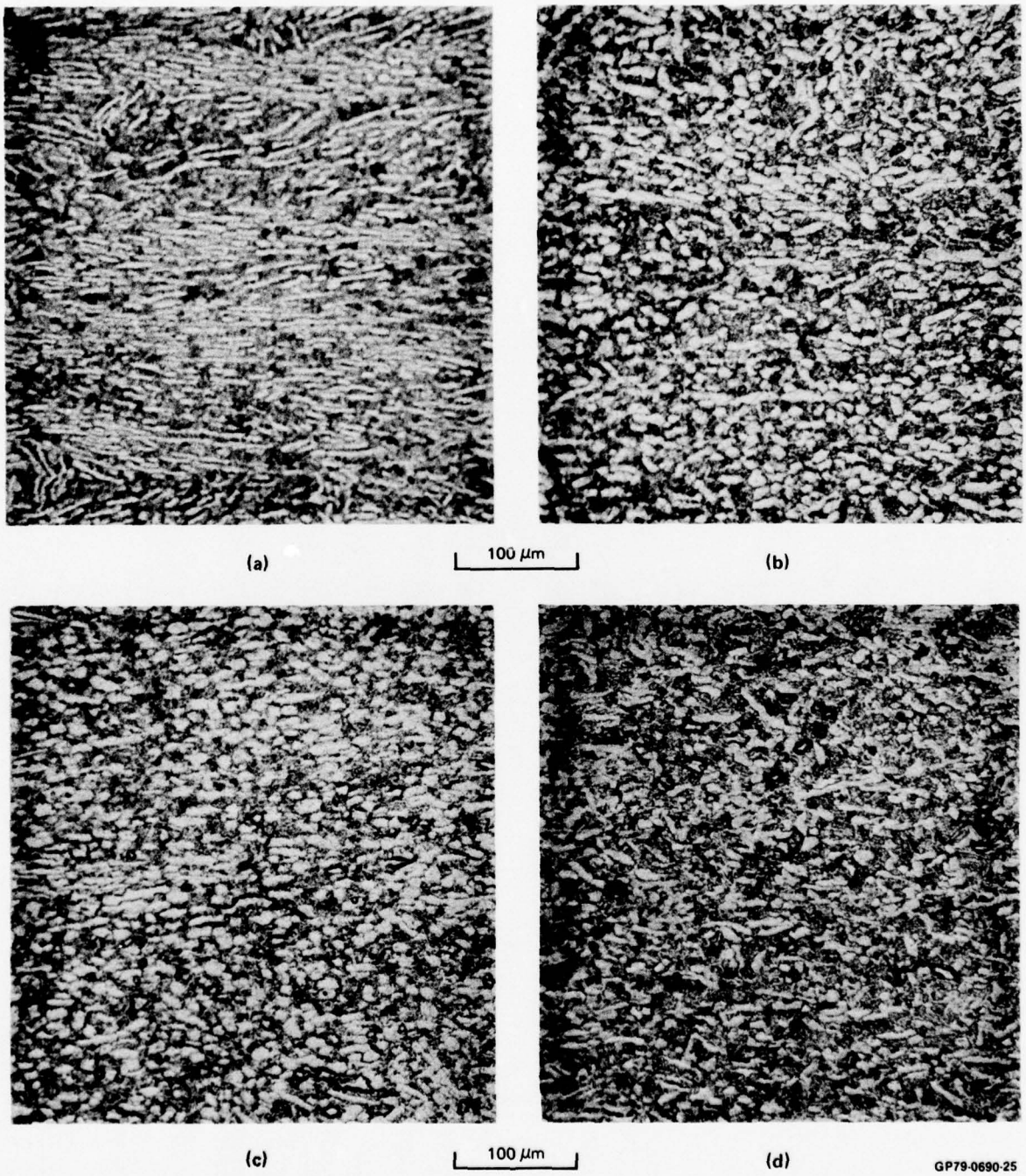

Figure 13. Microstructures of mill annealed Ti-6Al-4V and Ti-6Al-4V-0.1Er alloys; (a) 30-mm plate Ti-6Al-4V, (b) 30-mm plate Ti-6Al-4V-0.1Er, (c) 13-mm plate Ti-6Al-4V, and (d) 13-mm plate Ti-6Al-4V-0.1Er

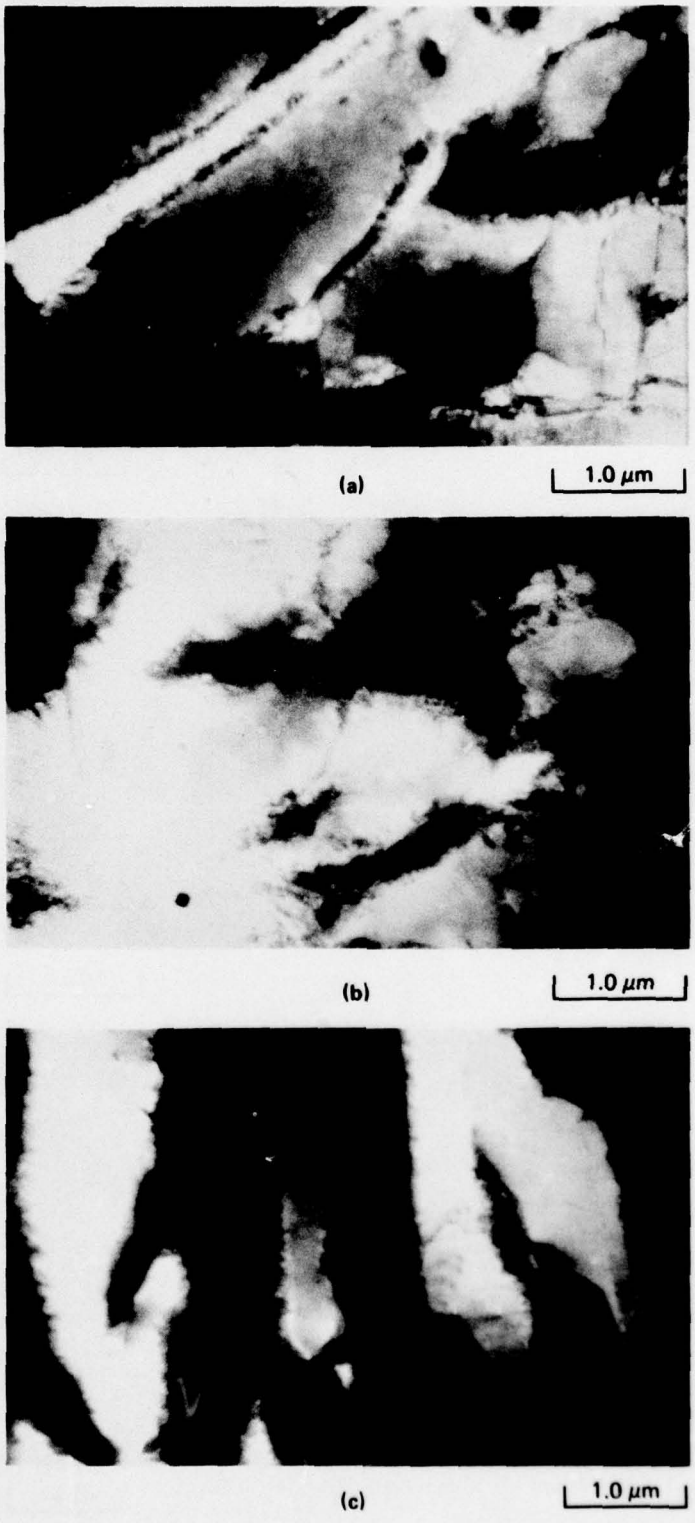

Figure 14. *Transmission electron micrographs of mill-annealed (a) Ti-6Al-4V reference alloy, (b) Ti-6Al-4V-0.05Y alloy, and (c) Ti-6Al-4V-0.1Er alloy*

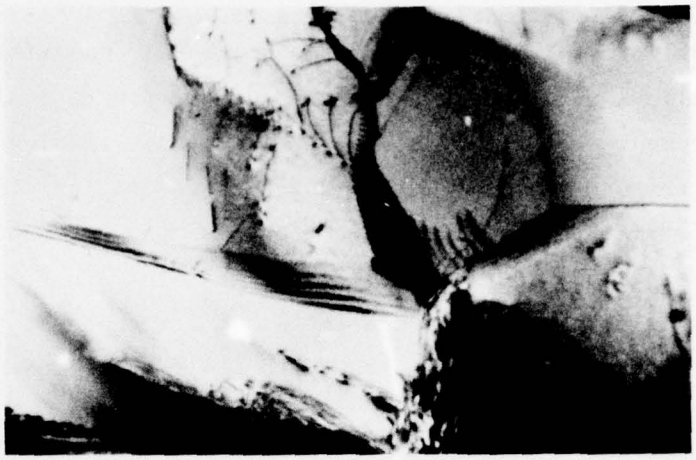

(a) 1.0 μm

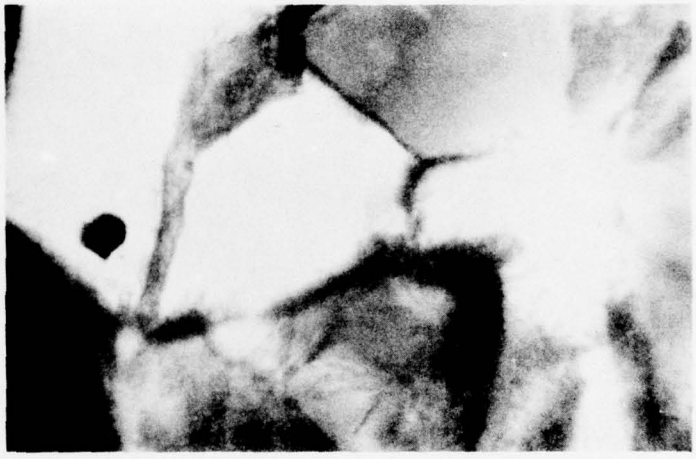

(b) 1.0 μm

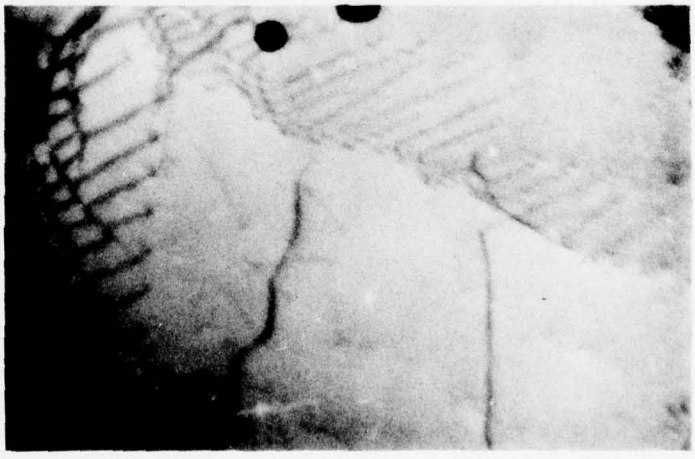

GP79-0690-27

(c) 0.5 μm

Figure 15. Transmission electron micrographs of recrystallization-annealed (a) Ti-6Al-4V reference alloy (b) Ti-6Al-4V-0.05Y alloy, (c) Ti-6Al-4V-0.1Er alloy

3.3 Crystallographic Texture of Phase III Ti-6Al-4V-RE Alloys

The crystallographic textures of the hot-worked and mill-annealed Ti-6Al-4V-RE alloys were determined by x-ray pole-figure goniometry. The texture development in the alloys was studied by determining the (0002) pole figures. The texture gradient in the thickness direction of 80-mm and 30-mm plates was determined from pole figures of specimens from the surface, quarter thickness, and mid-plane regions of the plates.

The 80-mm alloy plates have the intense multicomponent textures (Figure 16) expected from extensive forging in the beta field. The texture sharpnesses at the quarter-thickness and center planes are lower than at the surface (Figure 17). The 30-mm and 13-mm plates which were rolled in the alpha-beta field exhibit transverse-basal texture as shown in Figures 18 and 19. Mill annealing does not result in any significant changes in the texture (Figures 20 and 21). The deformation texture is unaffected by the rare-earth additives.

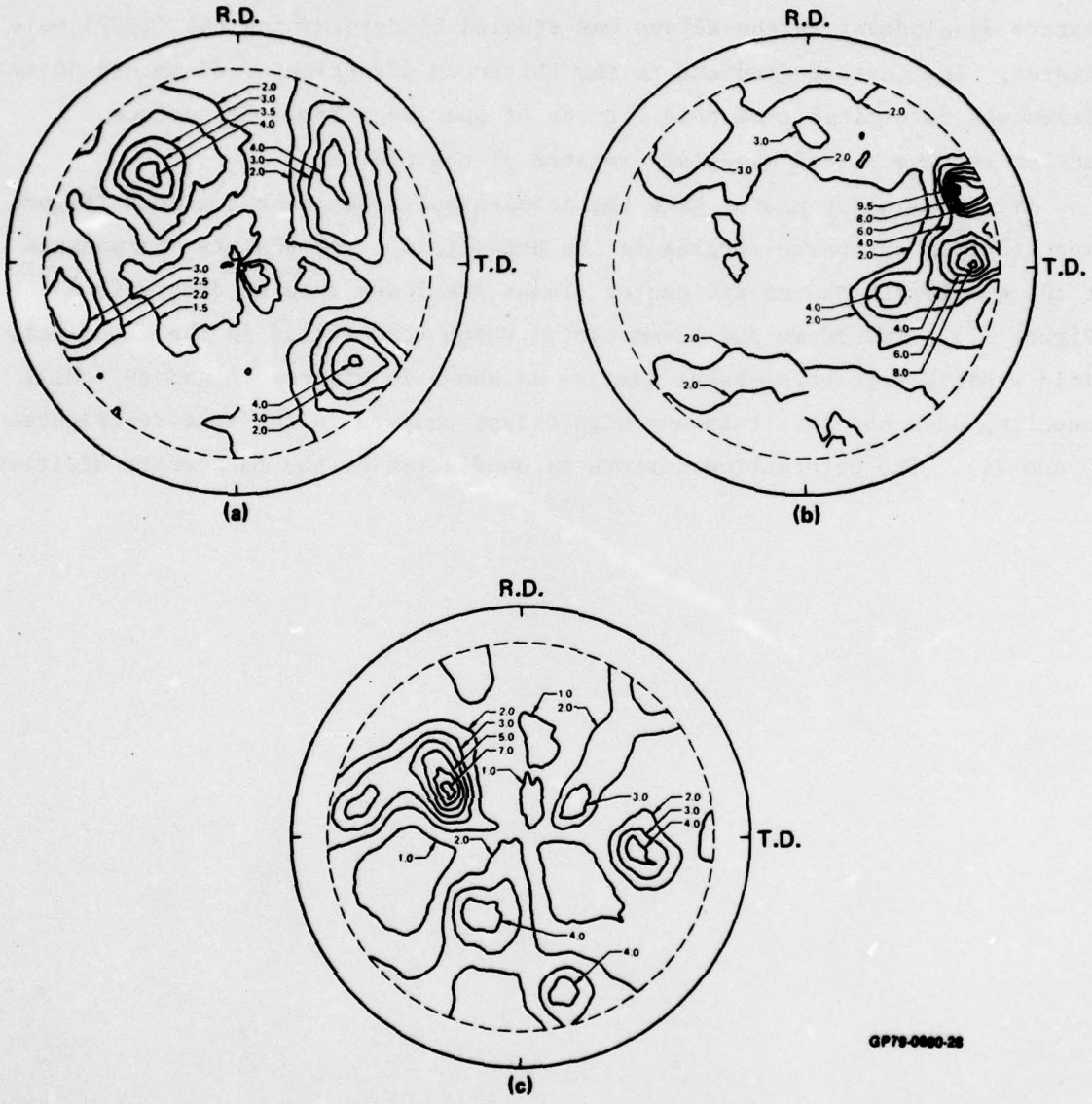

Figure 16. (0002) pole figures at quarter-thickness of 80-mm plates of (a) Ti-6Al-4V reference alloy, (b) Ti-6Al-4V-0.05Y, and (c) Ti-6Al-4V-0.1Er

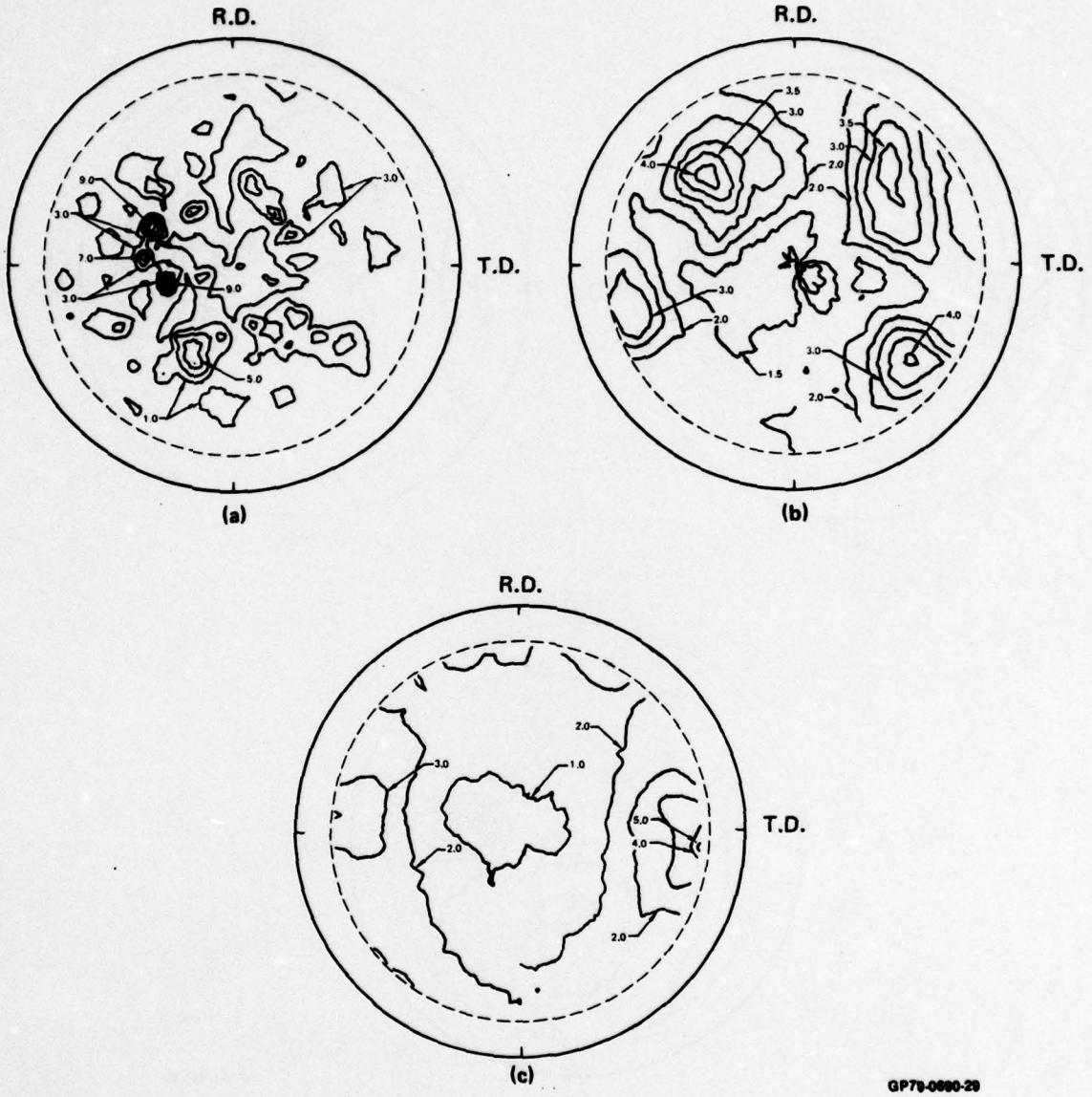

Figure 17. Texture gradient along thickness of 80-mm plate Ti-6Al-4V reference alloy; (0002) pole figure distribution at (a) surface, (b) quarter-thickness, and (c) center plane

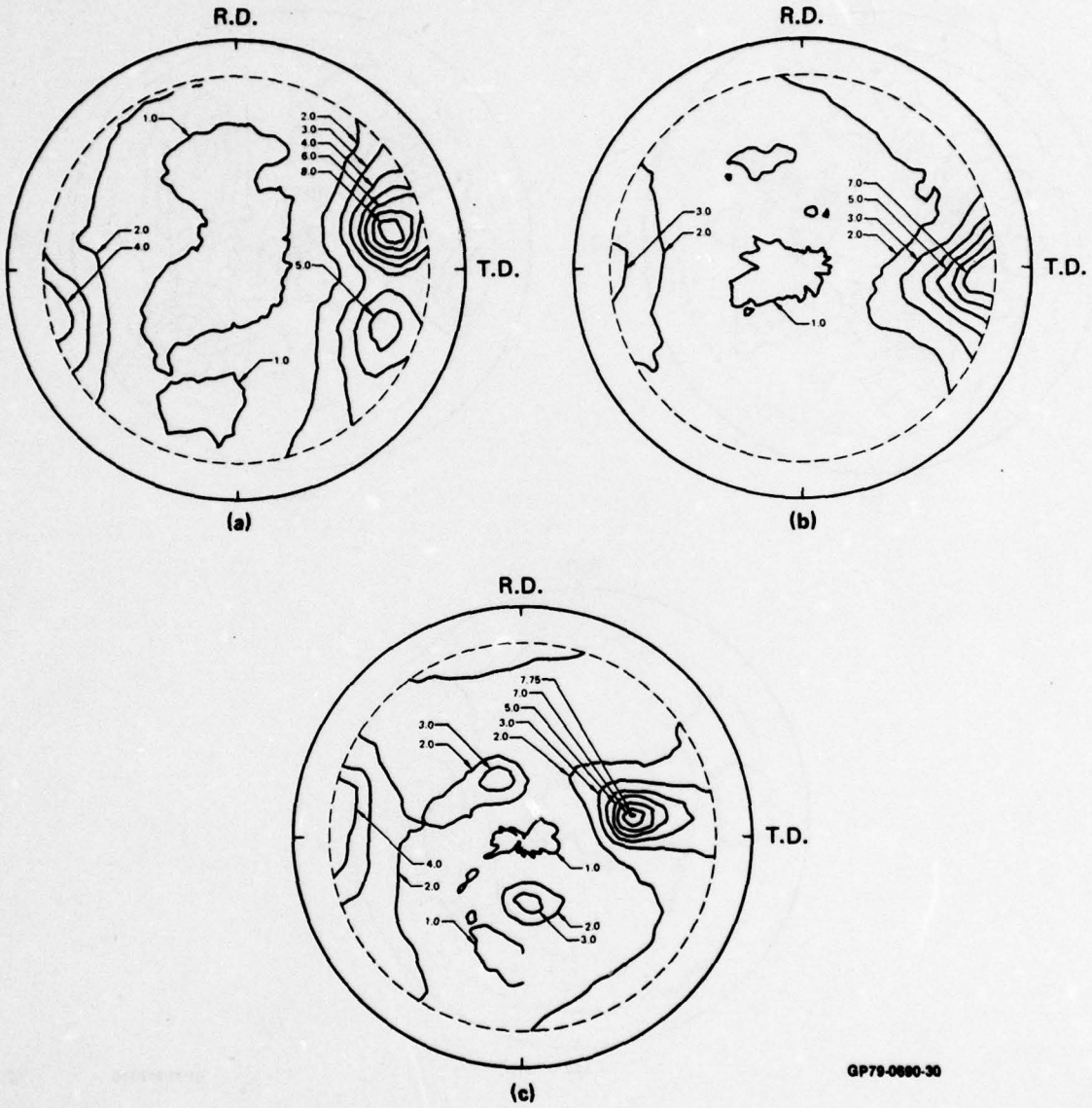

Figure 18. (0002) pole figures at half-thickness of 30-mm plates of (a) Ti-6Al-4V reference alloy, (b) Ti-6Al-4V-0.05Y, and (c) Ti-6Al-4V-0.1Er

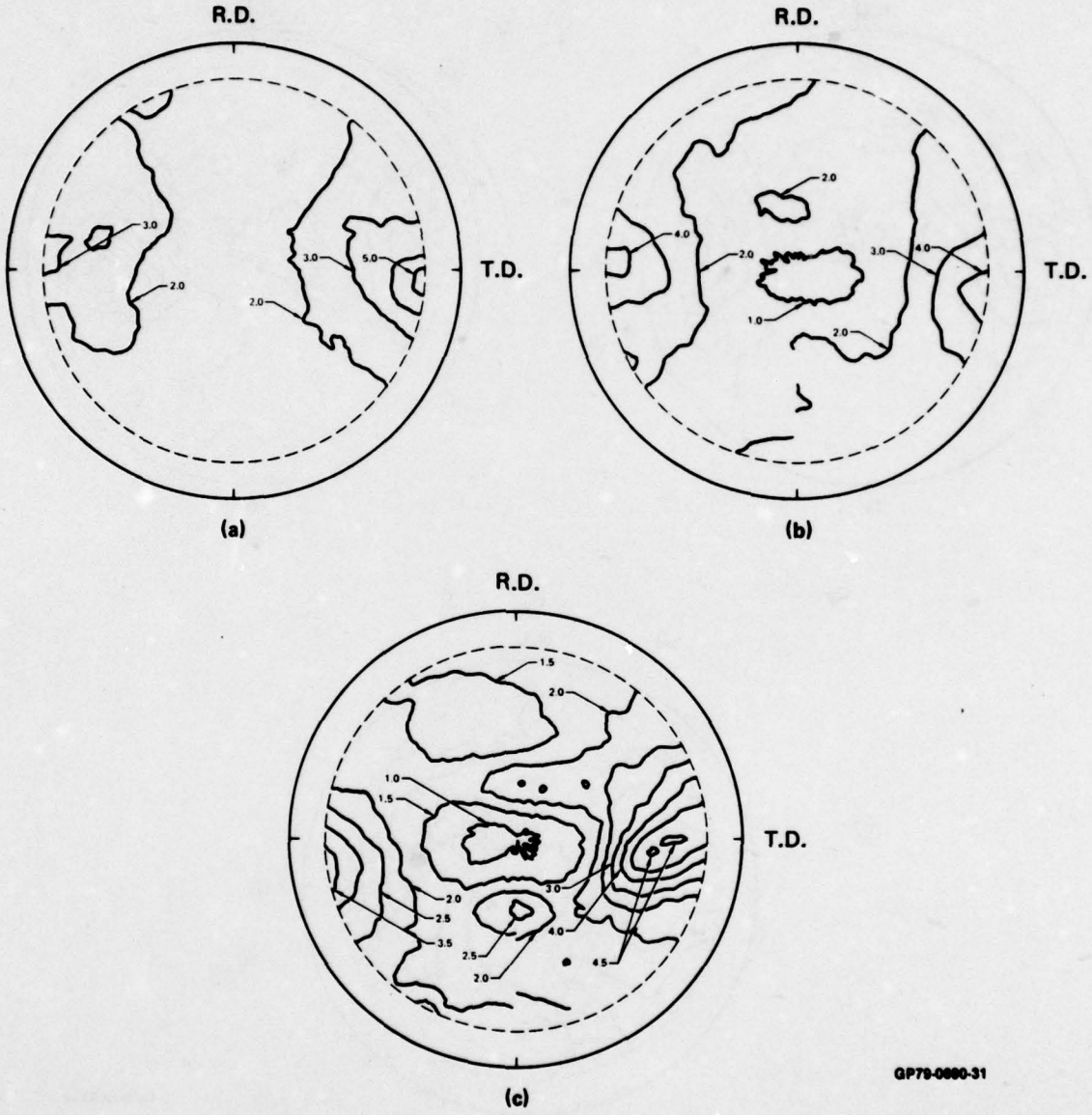

Figure 19. (0002) pole figures at half-thickness of 13-mm plates of (a) Ti-6Al-4V reference alloy, (b) Ti-6Al-4V-0.05Y, and (c) Ti-6Al-4V-0.1Er

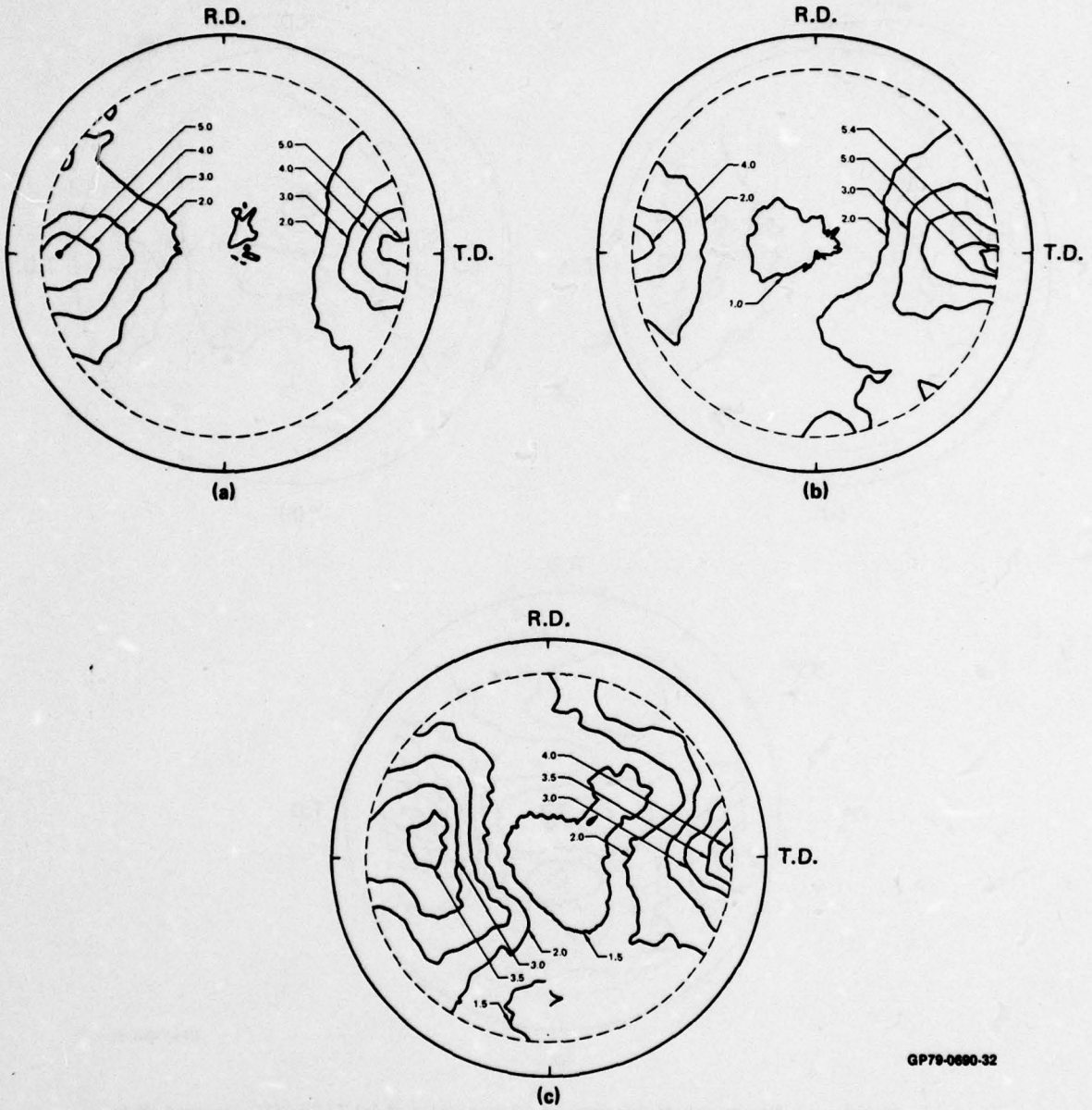

Figure 20. Effect of mill annealing on texture of 30-mm plate of (a) Ti-6Al-4V reference alloy, (b) Ti-6Al-4V-0.05Y, and (c) Ti-6Al-4V-0.1Er

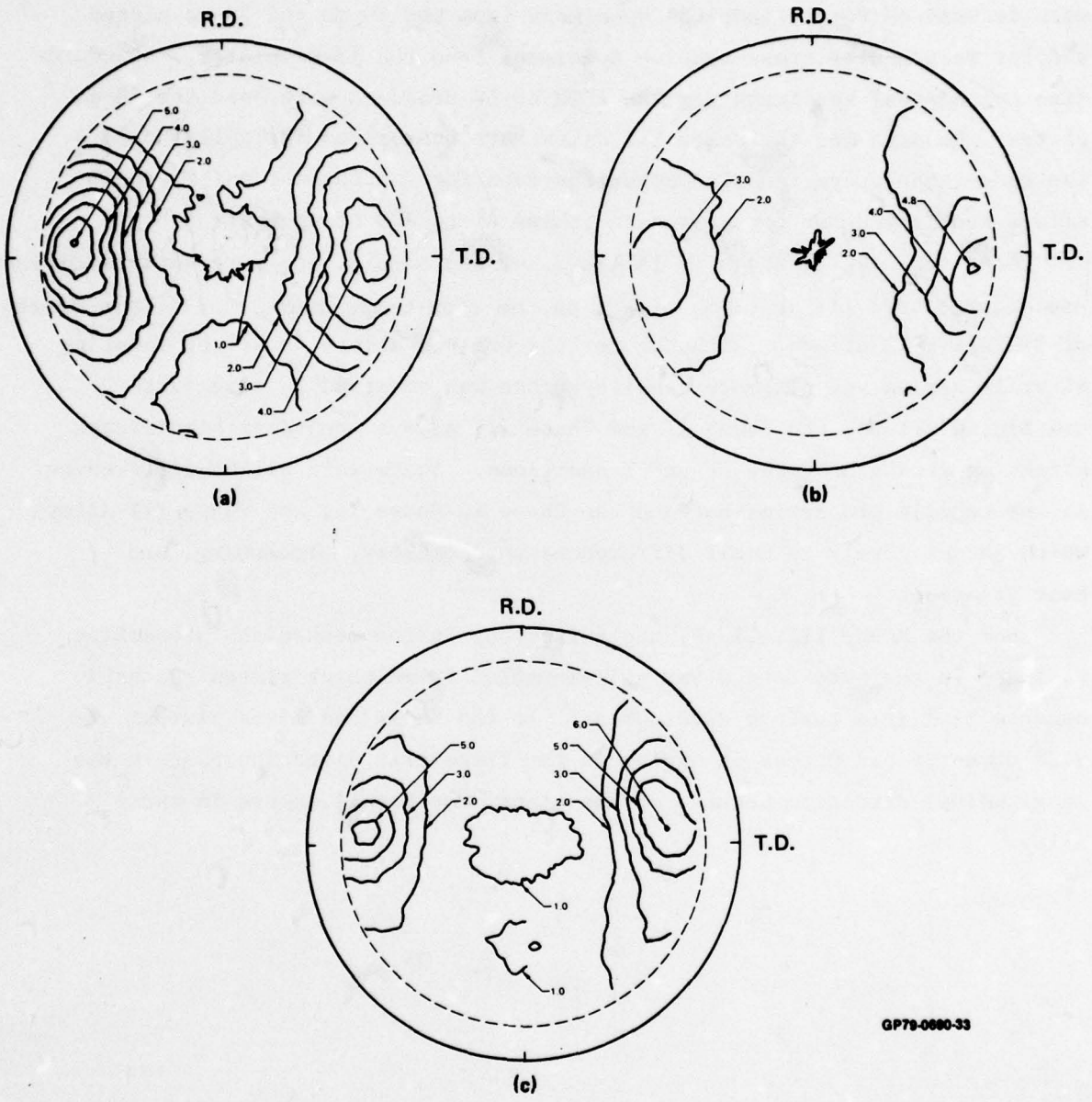

Figure 21. Effect of mill annealing on texture of 13-mm plate of (a) Ti-6Al-4V reference alloy, (b) Ti-6Al-4V-0.05Y, and (c) Ti-6Al-4V-0.1Er

4. ROOM-TEMPERATURE TENSILE PROPERTIES

The room-temperature mechanical properties of the Phase III alloys were determined for cylindrical specimens from the 80-mm and 30-mm plates and for rectangular cross-section specimens from the 13-mm plates. Standard-size cylindrical specimens per the ASTM E8-69 standard were used for 80-mm plates. Results for the Phase III alloys are summarized in Tables 3 and 4. The room-temperature tensile-properties data for the Phase I and Phase II alloys are listed for comparison in Tables A1 to A22 of Appendix A.

From the results shown in Tables 3, 4, and A1-A16, the rare-earth additives are seen to have little or no effect on the room-temperature tensile properties of Ti-6Al-4V-RE alloys. Although for the Phase I alloys, a slight lowering of yield stress and ultimate tensile stress was observed in rare-earth containing alloys, the Phase II and Phase III alloys showed no significant effect on strength by the Er and Y additions. There were slight differences in the tensile properties between the Phase I, Phase II, and Phase III alloys which is due likely to small differences in chemistry, processing, and heat treatment.

For the Phase III alloys, the anisotropy in the mechanical properties is least in the beta-forged and mill-annealed 80-mm thick plates, probably because of little texture development. In the 30-mm and 13-mm plates, the 0.2% offset yield stress is higher in the transverse direction than in the longitudinal direction because of the transverse basal texture in these alloys.

TABLE 3. ROOM-TEMPERATURE TENSILE PROPERTIES OF MILL-ANNEALED PHASE III Ti-6Al-4V-RE ALLOYS WITH LOAD IN LONGITUDINAL (L), TRANSVERSE (T), AND SHORT-TRANSVERSE (S-T) DIRECTIONS.

Alloy thickness and composition	Yield stress at 0.2% offset (MPa)			Ultimate tensile stress (MPa)			Uniform elongation (%)			Total elongation (%)		
	L	T	S-T	L	T	S-T	L	T	S-T	L	T	S-T
80-mm plate												
Ti-6Al-4V control	845	854	847	894	883	921	5.1	3.5	5.7	13.7	9.4	13.2
Ti-6Al-4V-0.1Er	825	829	838	867	882	915	4.8	6.5	5.7	10.6	7.8	10.7
Ti-6Al-4V-0.05Y	829	875	817	866	910	914	3.1	7.0	5.9	7.5	10.3	10.9
30-mm plate												
Ti-6Al-4V control	904	973		938	989		6.5	7.2		12.8	12.0	
Ti-6Al-4V-0.1Er	851	913		904	943		7.2	7.0		13.0	12.3	
Ti-6Al-4V-0.05Y	872	983		919	1012		6.8	7.5		11.4	12.5	
13- mm plate												
Ti-6Al-4V control	924	976		970	1009		6.2	6.0		18.4	17.1	
Ti-6Al-4V-0.1Er	865	952		924	1002		6.9	7.6		19.0	19.9	
Ti-6Al-4V-0.05Y	889	925		937	968		6.0	6.7		17.6	16.9	

GP79-0690-3

TABLE 4. ROOM-TEMPERATURE TENSILE PROPERTIES OF RECRYSTALLIZATION-ANNEALED PHASE III Ti-6Al-4V-RE ALLOYS WITH LOAD IN LONGITUDINAL (L), TRANSVERSE (T), AND SHORT-TRANSVERSE (S-T) DIRECTIONS.

Alloy thickness and composition	Yield stress at 0.2% offset (MPa)			Ultimate tensile stress (MPa)			Uniform elongation (%)			Total elongation (%)		
	L	T	S-T	L	T	S-T	L	T	S-T	L	T	S-T
80-mm plate												
Ti-6Al-4V control	837	836	845	891	873	873	3.4	2.9	4.2	9.4	8.5	9.3
Ti-6Al-4V-0.1Er	802	825	770	860	876	867	7.0	5.7	4.6	14.0	11.8	11.5
Ti-6Al-4V-0.05Y	770	836	781	822	869	855	5.6	6.5	6.0	8.6	9.3	8.4
30-mm plate												
Ti-6Al-4V control	839	943		901	981		7.8	9.2		13.0	13.9	
Ti-6Al-4V-0.1Er	829	875		887	915		6.1	7.8		12.2	12.9	
Ti-6Al-4V-0.05Y	847	894		911	931		7.6	8.1		13.6	12.8	
13-mm plate												
Ti-6Al-4V control	876	896		940	955		7.8	7.9		20.2	20.7	
Ti-6Al-4V-0.1Er	821	875		895	931		7.0	7.5		18.8	20.2	
Ti-6Al-4V-0.05Y	851	851		919	904		7.4	6.7		21.1	15.6	

GP79-0690-4

5. FRACTURE TOUGHNESS OF PHASE III Ti-6Al-4V-RE ALLOYS

The plane-strain fracture toughness (K_{IC}) of the 80-mm plates in the TL, LT, SL, LS, TS, and ST directions and of the 30-mm plates in the TL and LT directions was determined in accordance with ASTM standard E399-74 for the mill-anneal and recrystallization-anneal conditions. The fracture toughness (K_Q) of 30-mm and 13-mm plates was determined from three-point-loaded slow-bend tests of Charpy V-notched and fatigue-precracked specimens. The K_{IC} and K_Q values for Phase III alloys are given in Tables 5 and 6, and K_Q and plane-stress fracture toughness values of Phase II alloys are given in Tables 7 and 8.

TABLE 5. FRACTURE TOUGHNESS OF PHASE III Ti-6Al-4V-RE ALLOYS DETERMINED FROM SLOW-BEND TESTS OF FATIGUE-PRECRACKED CHARPY V-NOTCHED SPECIMENS.

Alloy thickness and composition	Specimen orientation[a]	Fracture toughness [MPa$\sqrt{m}$ (ksi$\sqrt{in.}$)]	
		Mill annealed	Recrystallization annealed
30-mm plate			
Ti-6Al-4V control	L-S	74 (68)	125 (114)
Ti-6Al-4V-0.1Er	L-S	87 (79)	100 (91)
Ti-6Al-4V-0.05Y	L-S	91 (82)	97 (88)
Ti-6Al-4V control	T-S	43 (39)	47 (42)
Ti-6Al-4V-0.1Er	T-S	55 (50)	92 (84)
Ti-6Al-4V-0.05Y	T-S	48 (44)	77 (70)
13-mm plate			
Ti-6Al-4V control	T-L	–	82 (74)
Ti-6Al-4V-0.1Er	T-L	–	101 (91)
Ti-6Al-4V-0.05Y	T-L	50 (45)	114 (103)
Ti-6Al-4V control	L-T	65 (59)	102 (93)
Ti-6Al-4V-0.1Er	L-T	114 (104)	135 (123)
Ti-6Al-4V-0.05Y	L-T	78 (71)	–

[a] First letter indicates load direction, and second letter indicates crack direction; L, T, and S are longitudinal, long-transverse, and short-transverse directions, respectively

GP79-0690-5

TABLE 6. PLANE-STRAIN FRACTURE TOUGHNESS OF PHASE III Ti-6Al-4V-RE ALLOYS.

Heat treatment	Alloy thickness and composition	K_{IC} (MPa·√m)					
		T-L	L-T	L-S	S-L	T-S	S-T
Mill anneal	80-mm plate						
	Ti-6Al-4V	84.7	82.7	95.9	78.4	93.0	76.0
	Ti-6Al-4V-0.05Y	60.1	62.2	87.7	57.4	83.1	63.0
	Ti-6Al-4V-0.1Er	–	67.5	90.6	72.3	85.0	68.4
	30-mm plate						
	Ti-6Al-4V	48.6	49.5	–	–	–	–
	Ti-6Al-4V-0.05Y	46.3	–	–	–	–	–
	Ti-6Al-4V-0.1Er	53.6	50.3	–	–	–	–
Recrystallization anneal	80-mm plate						
	Ti-6Al-4V	75.2	76.8	–	86.8	100.4	85.8
	Ti-6Al-4V-0.05Y	68.3	75.7	86.9	76.8	105.6	65.6
	Ti-6Al-4V-0.1Er	70.2	73.8	97.2	74.8	90.1	75.9
	30-mm plate						
	Ti-6Al-4V	58.5	57.8	–	–	–	–
	Ti-6Al-4V-0.05Y	62.3	69.4	–	–	–	–
	Ti-6Al-4V-0.1Er	73.8	73.4	–	–	–	–

GP79-0690-6

TABLE 7. FRACTURE TOUGHNESS VALUES (K_Q) DETERMINED FROM SLOW-BEND, PRECRACKED, CHARPY SAMPLES OF PHASE II Ti-6Al-4V-RE ALLOYS

Alloy composition	Rolling schedule	K_Q [MPa√m (ksi√in.)]								
		Recrystallization annealed			Beta annealed			Solution-treat-and-aged		
		T-L	L-T	T-S	T-L	L-T	T-S	T-L	L-T	T-S
Ti-6Al-4V	A	84.7 (77)	92.4 (84)	115.5 (105)	85.8 (78)	96.8 (88)	90.2 (82)	–	46.2 (42)	50.6 (46)
	B	127.6 (116)	94.6 (86)	116.6 (106)	94.6 (86)	85.8 (78)	89.1 (81)	52.8 (48)	–	51.7 (47)
Ti-6Al-4V-0.02Y	A	85.8 (78)	81.4 (74)	100.1 (91)	71.5 (65)	81.4 (74)	70.4 (64)	42.9 (39)	46.2 (42)	45.1 (41)
	B	86.9 (79)	95.7 (87)	86.9 (79)	69.3 (63)	74.8 (68)	72.6 (66)	33.0 (30)	41.8 (38)	40.7 (37)
Ti-6Al-4V-0.05Y	A	80.3 (73)	–	96.8 (88)	58.3 (53)	75.9 (69)	59.4 (54)	37.4 (34)	33.0 (30)	40.7 (37)
	B	63.8 (58)	89.1 (81)	77.0 (70)	58.3 (53)	72.6 (66)	62.7 (57)	40.7 (37)	49.5 (45)	35.2 (32)
Ti-6Al-4V-0.10Er	A	75.9 (69)	83.6 (76)	78.1 (71)	63.8 (58)	72.6 (66)	72.6 (66)	44.0 (40)	–	42.9 (39)
	B	91.3 (83)	101.2 (92)	115.5 (105)	72.6 (66)	80.3 (73)	68.2 (62)	42.9 (39)	45.1 (41)	44.0 (40)
Ti-6Al-4V-0.038Y_2O_3	A	82.5 (75)	90.2 (82)	141.9 (129)	70.4 (64)	81.4 (74)	75.9 (69)	44.0 (40)	38.5 (35)	–
	B	–	102.3 (93)	92.4 (84)	73.7 (67)	77.0 (70)	75.9 (69)	33.0 (30)	45.1 (41)	45.1 (45)

Processing condition: A = continuously rolled from 26 mm to 13 mm thickness from 940°C
B = continuously rolled from 26 mm to 13 mm thickness from 1025°C

GP79-0690-7

TABLE 8. PLANE-STRESS FRACTURE TOUGHNESS VALUES DETERMINED FROM CENTER-CRACKED TENSION SPECIMENS OF PHASE II Ti-6Al-4V-RE ALLOYS

Alloy	Alloy composition	Rolling schedule	Fracture toughness K_Q [MPa $\sqrt{m}$ (ksi $\sqrt{in.}$)]		
			Beta annealed	Recrystallization annealed	Solution-treat-and-aged
31	Ti-6Al-4V	A	132 (120)	130 (118)	143 (130)
		B	140 (127)	–	151 (137)
33	Ti-6Al-4V-0.02Y	A	154 (140)	123 (112)	136 (124)
		B	153 (139)	–	121 (110)
34	Ti-6Al-4V-0.05Y	A	152 (138)	123 (112)	–
		B	158 (144)	–	139 (126)
32	Ti-6Al-4V-0.10Er	A	165 (150)	130 (118)	134 (122)
		B	154 (140)	–	136 (124)
36	Ti-6Al-4V-0.038Y_2O_3	A	161 (146)	134 (122)	129 (117)
		B	143 (130)	–	150 (136)

Processing condition: A = continuously rolled from 26 mm to 13 mm thickness from 940°C
B = continuously rolled from 26 mm to 13 mm thickness from 1025°C

GP78-0635-14

The high K_{IC} values of 80-mm plates are as expected for beta processing. Because the 80-mm plates are only lightly worked, they are not microstructurally uniform throughout. Consequently, any apparent differences in K_{IC} values of the three alloys are likely due to microstructural variations rather than rare-earth effects. The 30-mm plates, on the other hand, have undergone significant hot working and have uniform microstructures. The results for the 30-mm plates indicate that Er and Y additions increase the K_{IC} of Ti-6Al-4V in the recrystallization-annealed condition.

From the data shown in Tables 5-8, it can be concluded that the fracture toughness of Ti-6Al-4V is not adversely affected by Er and Y additives. The small differences observed between the reference and rare-earth containing alloys are within the experimental scatter-band characteristic of fracture toughness measurements. In the instances where large differences are observed, the Y- and Er-containing alloys have higher fracture toughness than the reference alloy.

6. HIGH-TEMPERATURE DEFORMATION OF PHASE III Ti-6Al-4V-RE ALLOYS

6.1 High-Temperature, High-Strain-Rate Deformation of Phase III Ti-6Al-4V-RE Alloys

High-temperature compression tests were performed on cast, mill-annealed, and recrystallization-annealed Phase III alloys at 750, 885, and 925°C at strain rates of 0.005-0.5 s^{-1}. Cylindrical specimens of 8.9-mm diam and 12-mm height were compressed between flat faces of 60-mm diam stainless-steel compression rams. The specimens were heated to the desired temperature in a three-zone, resistance-wound, split furnace and maintained at temperature for 10 min before compression was begun. Flow stresses were calculated from the deformation load, and ram displacement was recorded by an x-y plotter.

The strain rate and temperature dependences of flow stress of the Ti-6Al-4V-RE alloys are shown in Tables 9 and 10 and Figures 22-24. The Er and Y additions reduce the flow stress of Ti-6Al-4V by 5-10% at strain rates of 0.005 s^{-1} and 0.05 s^{-1}. The effect of Er and Y additions on the high-temperature flow stress decreases with increasing prior hot-working. Thus, for the 30-mm and 13-mm plates, no significant effect of Er and Y on flow stress is observed. From the flow-stress/strain-rate measurements, the strain-rate sensitivity, $m = [\partial \ln\sigma / \partial \ln\dot{\varepsilon}]$, was evaluated at different temperatures. The Y and Er additions have no significant effect on m.

6.2 Superplasticity of Phase III Ti-6Al-4V-RE Alloys

The effect of Y additions on the superplastic behavior of Ti-6Al-4V was studied by determining the strain-rate dependence of flow stress and strain-rate sensitivity. Figures 25a and 25b show the flow stress as a function of strain rate and the strain-rate dependence of m determined by strain-rate cycling tests for Ti-6Al-4V and Ti-6Al-4V-0.05Y. The Y-containing alloy exhibits a lower flow stress and higher m, and consequently better superplasticity than the reference alloy at strain rates of 10^{-5}-10^{-3} s^{-1}. The beneficial effects of the Y addition on the superplasticity of Ti-6Al-4V are due to the effectiveness of Y precipitates in retarding elevated-temperature grain growth, which is an essential requirement for superplastic behavior.

TABLE 9. HIGH-TEMPERATURE COMPRESSION TEST RESULTS OF MILL-ANNEALED PHASE III Ti-6Al-4V-RE ALLOYS.

Alloy thickness and composition	Yield stress (MPa)								
	T = 750°C			T = 885°C			T = 925°C		
	Strain rate (s^{-1})			Strain rate (s^{-1})			Strain rate (s^{-1})		
	$\dot{\epsilon}$ = 0.005	$\dot{\epsilon}$ = 0.05	$\dot{\epsilon}$ = 0.5	$\dot{\epsilon}$ = 0.005	$\dot{\epsilon}$ = 0.05	$\dot{\epsilon}$ = 0.5	$\dot{\epsilon}$ = 0.005	$\dot{\epsilon}$ = 0.05	$\dot{\epsilon}$ = 0.5
80-mm plate									
Ti-6Al-4V control	224	304	430	77	135	207	54	81	132
Ti-6Al-4V-0.1Er	234	308	441	69	113	206	46	77	138
Ti-6Al-4V-0.05Y	184	303	428	71	119	194	39	70	133
30-mm plate									
Ti-6Al-4V control	259	365	496	–	136	212	47	80	131
Ti-6Al-4V-0.1Er	244	333	456	67	119	205	41	72	121
Ti-6Al-4V-0.05Y	242	326	–	68	118	197	43	79	123
13-mm plate									
Ti-6Al-4V control	244	349	472	65	117	185	45	74	127
Ti-6Al-4V-0.1Er	251	348	479	71	122	208	41	73	125
Ti-6Al-4V-0.05Y	230	332	456	61	109	197	41	76	119

GP79-0690-8

TABLE 10. HIGH-TEMPERATURE COMPRESSION TEST RESULTS OF RECRYSTALLIZATION-ANNEALED PHASE III Ti-6Al-4V-RE ALLOYS.

Alloy thickness and composition	Yield stress (MPa)								
	T = 750°C			T = 885°C			T = 925°C		
	Strain rate (s^{-1})			Strain rate (s^{-1})			Strain rate (s^{-1})		
	$\dot{\epsilon}$ = 0.005	$\dot{\epsilon}$ = 0.05	$\dot{\epsilon}$ = 0.5	$\dot{\epsilon}$ = 0.005	$\dot{\epsilon}$ = 0.05	$\dot{\epsilon}$ = 0.5	$\dot{\epsilon}$ = 0.005	$\dot{\epsilon}$ = 0.05	$\dot{\epsilon}$ = 0.5
80-mm plate									
Ti-6Al-4V control	249	311	452	90	129	217	47	82	131
Ti-6Al-4V-0.1Er	247	271	458	83	123	204	47	75	126
Ti-6Al-4V-0.05Y	250	282	440	87	124	201	47	76	127
30-mm plate									
Ti-6Al-4V control	248	–	479	91	137	234	62	85	142
Ti-6Al-4V-0.1Er	231	262	444	76	120	220	51	73	121
Ti-6Al-4V-0.05Y	235	269	456	83	128	212	59	74	130
13-mm plate									
Ti-6Al-4V control	232	–	451	83	124	214	54	71	127
Ti-6Al-4V-0.1Er	236	301	436	76	117	208	51	64	118
Ti-6Al-4V-0.05Y	218	278	425	77	113	197	49	68	113

GP79-0690-9

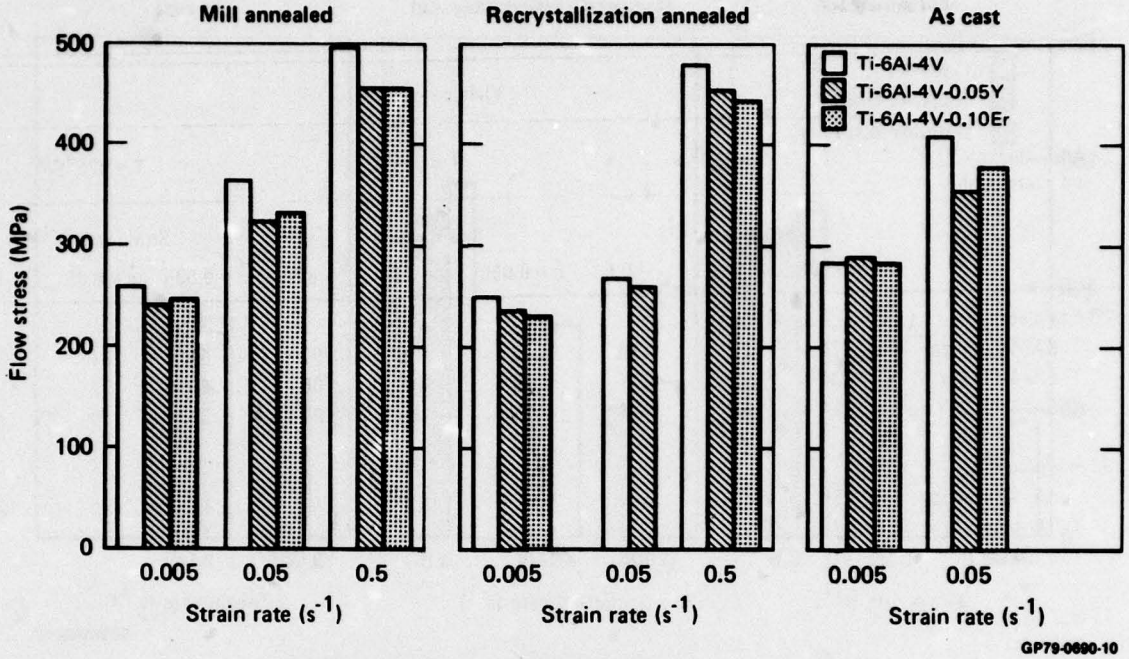

Figure 22. Flow stress of Ti-6Al-4V-RE alloys at 750°C

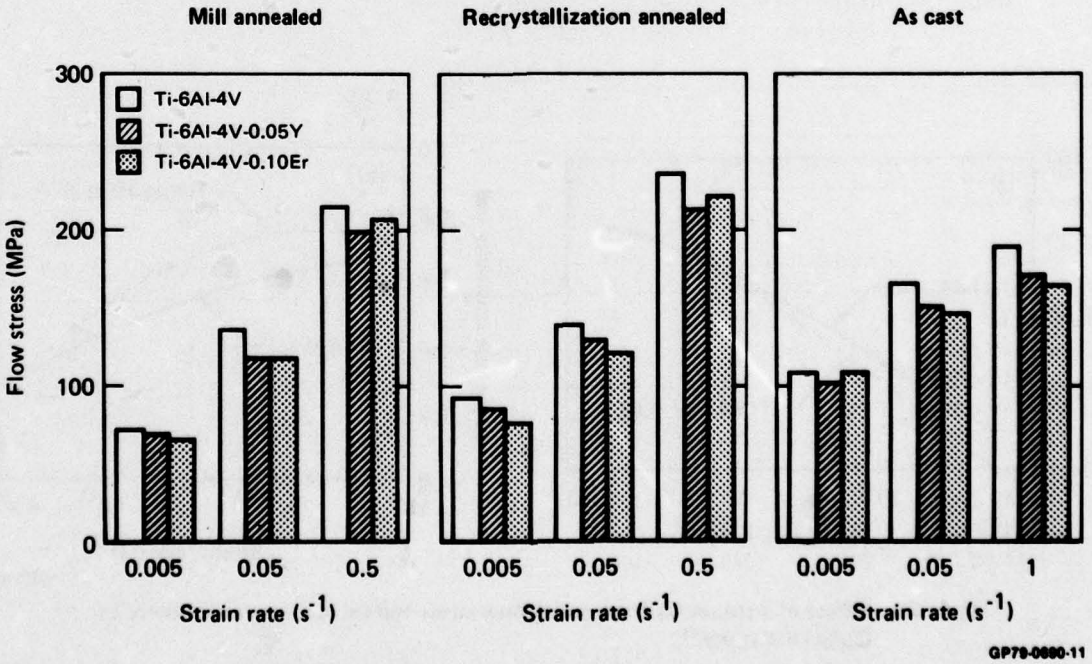

Figure 23. Flow stress of Ti-6Al-4V-RE alloys at 885°C

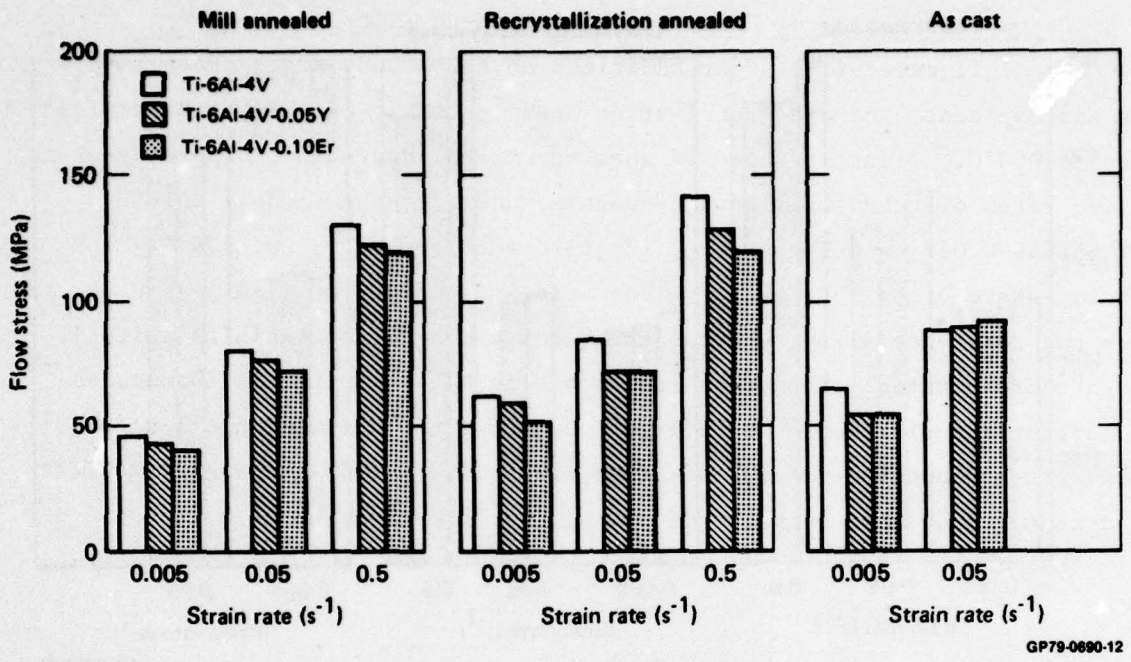

Figure 24. Flow stress of Ti-6Al-4V-RE alloys at 925°C

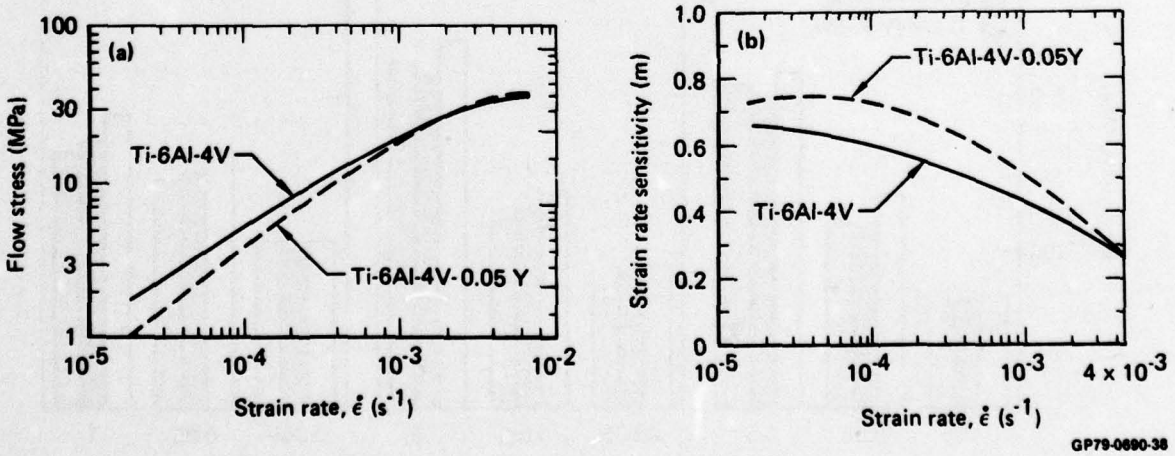

Figure 25. Effect of yttrium addition on (a) flow stress and (b) strain-rate sensitivity of Ti-6Al-4V at 906°C

6.3 Creep Deformation of Phase III Ti-6Al-4V-RE Alloys

The influence of Y and Er additions on the steady-state creep rate, stress exponent, and creep activation energies of Ti-6Al-4V was determined at 350-600°C. Figures 26 and 27 show the stress dependence of steady-state creep rates of recrystallization-annealed and mill-annealed Ti-6Al-4V, Ti-6Al-4V-0.05Y, and Ti-6Al-4V-0.1Er alloys at 500, 550, and 600°C. The steady-state creep rate at any given stress is lower for Ti-6Al-4V-0.1Er than for the reference alloy, whereas the Y-containing alloy exhibits slightly higher creep rates. The creep resistance is higher in the mill-annealed condition than in the recrystallization-annealed condition in all alloys. The stress dependence of steady-state creep rate follows a power law with exponent ≈ 3 at low stresses and ≈ 9 at high stresses.

The effect of orientation on stress dependence is shown in Figure 28. The alloys are more creep resistant when the stress direction is parallel to <0001> (long transverse direction) than when the stress is in the longitudinal direction. This is because of the higher critical resolved shear stress for <c+a> slip (<11$\bar{2}$3> slip) and a low Schmidt factor for 'a' slip in the <0001> orientation.

The temperature dependence of the steady-state creep rate at 164 MPa and 330 MPa is shown in Figure 29 for recrystallization-annealed Ti-6Al-4V-RE alloys. The activation energy (ΔH) of 188 kJ/mol observed at low stresses at 450-600°C agrees with the activation energy for self-diffusion in titanium, and hence creep in this region is controlled by dislocation climb. The rate-controlling creep mechanism associated with the high activation energy at higher stresses, however, is not clear at present. The Er and Y additions do not alter the stress exponent and activation energy significantly.

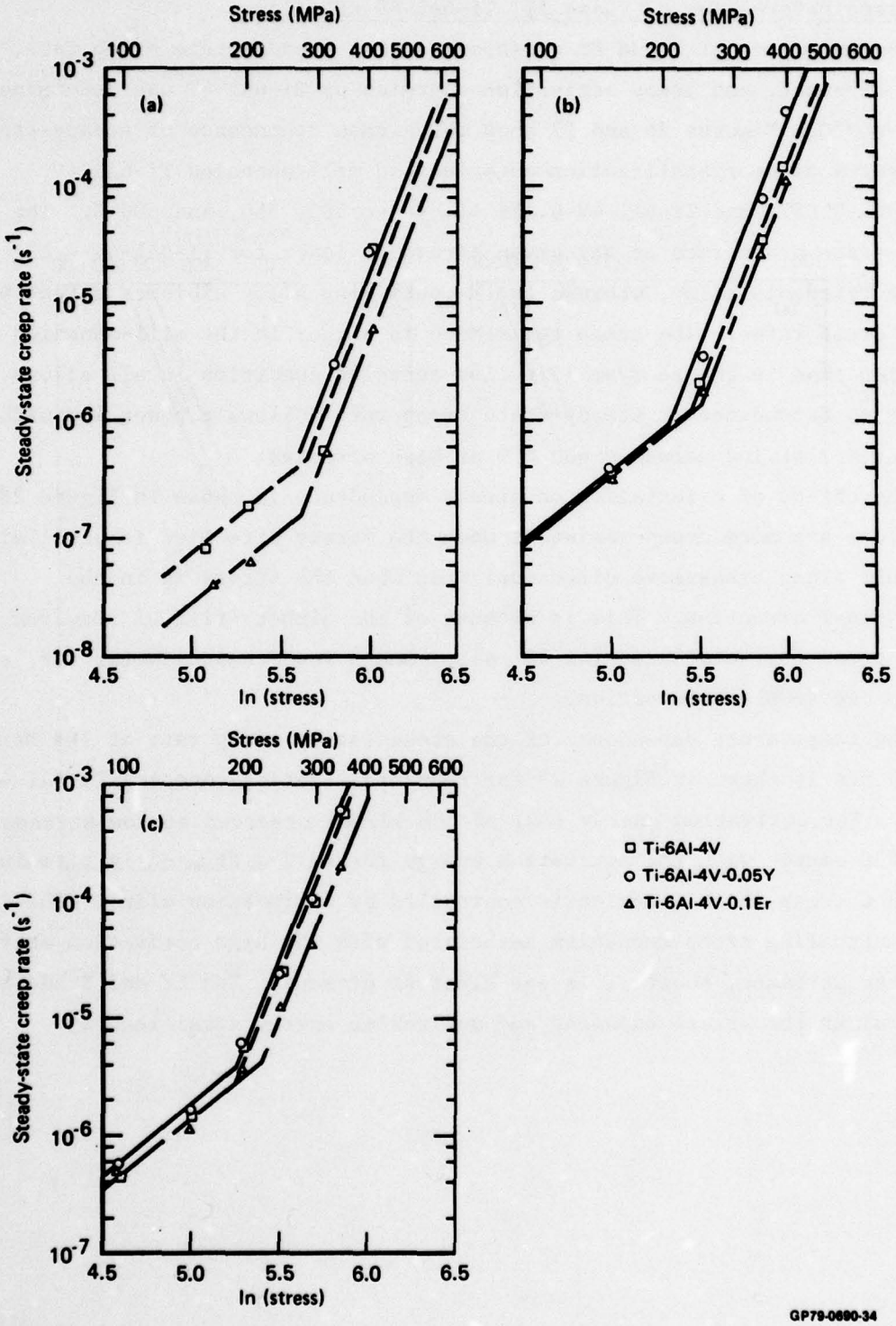

Figure 26. *Stress dependence of steady-state creep rate for recrystallization-annealed* Ti-6Al-4V-RE alloys at (a) 500°C, (b) 550°C, and (c) 600°C

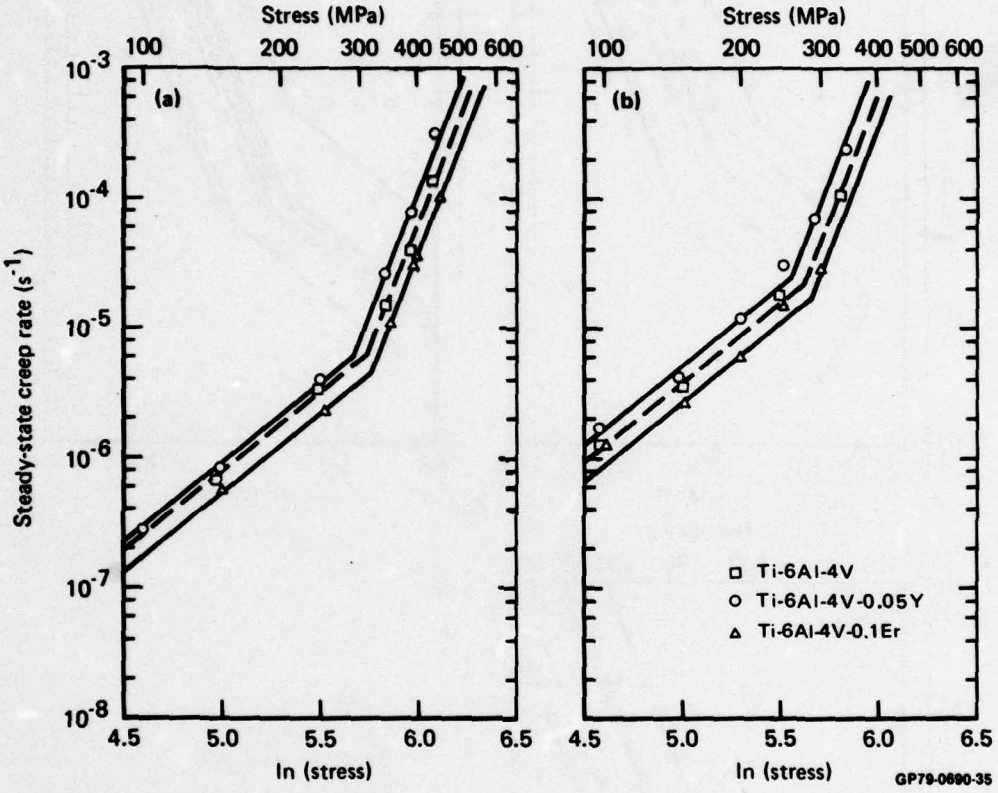

Figure 27. Stress dependence of steady-state creep rate for mill-annealed Ti-6Al-4V-RE alloys at (a) 550°C and (b) 600°C

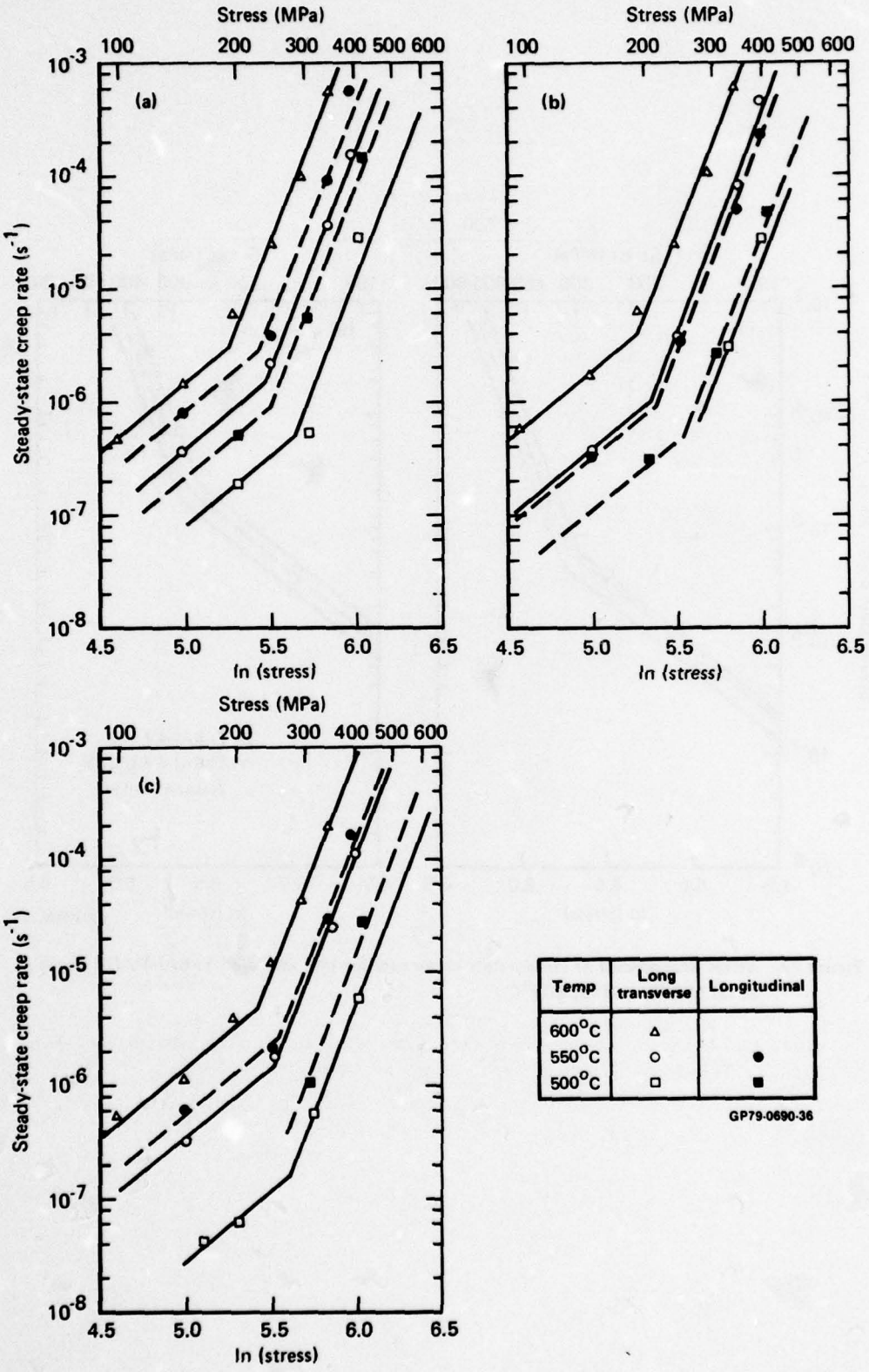

Figure 28. Effect of orientation on stress and temperature dependence of steady-state creep rate for (a) Ti-6Al-4V, (b) Ti-6Al-4V-0.05Y, and (c) Ti-6Al-4V-0.1Er

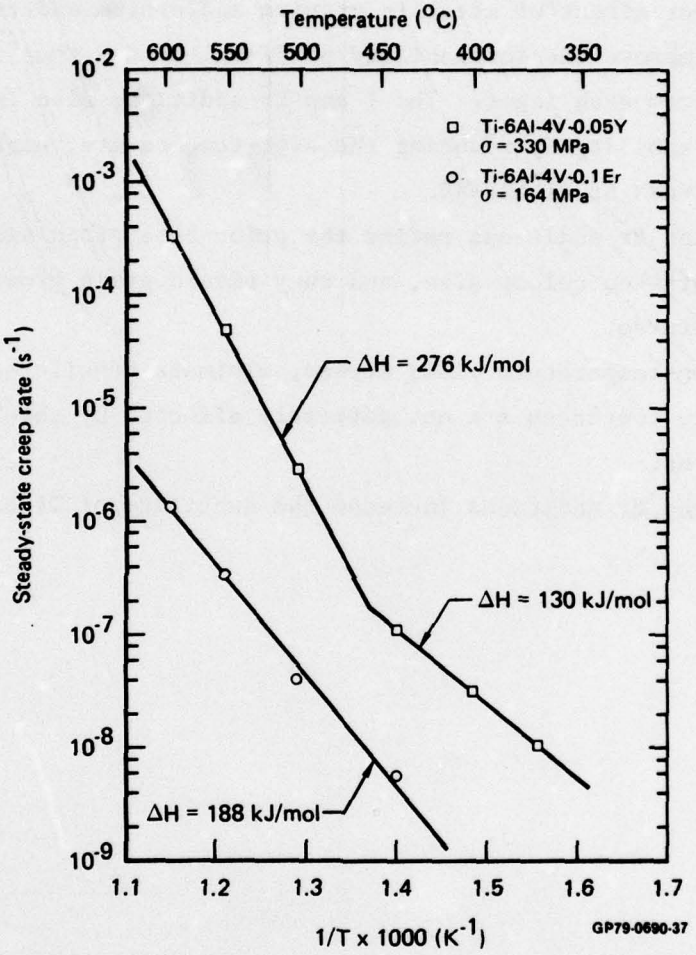

Figure 29. Temperature dependence of steady-state creep rate for recrystallization-annealed Ti-6Al-4V-RE alloys

7. CONCLUSIONS

Based on the results of Phases I, II, and III of the study, the following conclusions are drawn:

1. The major effect of metallic yttrium and erbium additions to Ti-6Al-4V is to improve the forgeability of Ti-6Al-4V and thus increase the yield from each ingot. The Y and Er additions also improve the hot workability by reducing the high-temperature, high-strain-rate flow stress of Ti-6Al-4V.
2. The Y and Er additions refine the prior-beta grain size and Widmanstätten colony size, and they retard grain growth at elevated temperatures.
3. The room-temperature yield stress, ultimate tensile stress, and fracture toughness are not adversely affected by the Y and Er additions.
4. The Y and Er additions increase the ductility of Ti-6Al-4V.

REFERENCES

1. C. R. Whitsett, S. M. L. Sastry, J. E. O'Neal, and R. J. Lederich, Influence of Rare-Earth Additions on Properties of Titanium Alloys: Microstructures and Room-Temperature Tensile Properties of Ti-6Al-4V with Yttrium, Erbium, and Mischmetal Additions, Technical Report for period 1 April 1976 - 31 March 1977 for ONR contract N00014-76-C-0626, McDonnell Douglas Report MDC Q0627 (31 May 1977).
2. C. R. Whitsett, S. M. L. Sastry, J. E. O'Neal, and R. J. Lederich, Influence of Rare-Earth Additions on Properties of Titanium Alloys: Room-Temperature Tensile Properties and Fracture Toughness of Ti-6Al-4V with Erbium, Yttrium, and Yttria Additions, Technical Report for period 1 April 1977 - 31 March 1978 for ONR contract N00014-76-C-0626, McDonnell Douglas Report MDC Q0654 (31 May 1978).
3. M. J. Buczek, G. S. Hall, S. R. Seagle, and H. B. Bomberger, Grain Refinement of Titanium Alloys, AFML-TR-74-255, November 1974.
4. B. B. Rath, R. J. Lederich, and J. E. O'Neal, Recrystallization and Grain Growth in Ti-Rare-Earth Alloy, ASM-AIME Materials Science Symposium, Cincinnati, OH, November 1975.
5. B. B. Rath, R. J. Lederich, and J. E. O'Neal, The Effects of Rare-Earth Additions on the Grain Refinement of Ti, in Grain Boundaries in Engineering Materials, ed. by J. L. Walter, J. H. Westbrook, and D. A. Woodford (Claitors Publ. Div., Baton Rouge, LA, 1975), p. 39.
6. B. B. Rath, J. E. O'Neal, and R. J. Lederich, Grain Refinement in Ti-Er Alloys, in Proc. Electron Microscopy Soc. Am., ed. by C. J. Arceneaux, (Claitors Publ. Div., Baton Rouge, LA, 1974), p. 522.

APPENDIX A. ROOM-TEMPERATURE TENSILE PROPERTIES OF Ti-6Al-4V-RE ALLOYS

Tables A1-A22 list the room-temperature tensile properties for the Ti-6Al-4V reference alloy, Ti-6Al-4V-Y, Ti-6Al-4V-Er, Ti-6Al-4V-MM, and Ti-6Al-4V-Y_2O_3 alloys that were determined in Phases I and II of this contract.

TABLE A1. ROOM-TEMPERATURE TENSILE PROPERTIES OF PHASE I Ti-6Al-4V-RE ALLOYS ANNEALED AT T_β – 56°C FOR 15 min

Alloy composition	Annealing temperature, T_β – 56°C (°C)	Elastic modulus (GPa)	Yield stress at 0.2% offset (MPa)	Ultimate tensile stress (MPa)	Fracture stress (MPa)	Uniform elongation (%)	Total elongation (%)
Ti-6Al-4V	954	136	965	1005	860	5.5	14.4
Ti-6Al-4V-0.020Y	954	137	945	985	840	5.0	13.0
Ti-6Al-4V-0.050Y	932	124	825	905	780	4.4	9.3
Ti-6Al-4V-0.10Y	932	129	870	940	760	6.0	13.5
Ti-6Al-4V-0.30Y	932	140	900	940	790	5.7	13.2
Ti-6Al-4V-0.010MM	932	123	845	920	795	6.1	12.9
Ti-6Al-4V-0.030MM	932	128	840	900	770	4.8	12.9
Ti-6Al-4V-0.080MM	932	137	890	930	825	6.4	13.3
Ti-6Al-4V-0.10Er	948	139	930	995	815	5.5	16.1
Ti-6Al-4V-0.30Er	926	103	870	910	760	5.1	14.0
Ti-6Al-4V-0.80Er (Ingot 27)	926	144	855	965	760	4.9	13.2
Ti-6Al-4V-0.80Er (Ingot 29)	926	129	875	905	720	5.9	14.2

GP77-0480-22

TABLE A2. ROOM-TEMPERATURE TENSILE PROPERTIES OF PHASE I Ti-6Al-4V-RE ALLOYS ANNEALED AT T_β – 56°C FOR 30 min

Alloy composition	Annealing temperature, T_β – 56°C (°C)	Elastic modulus (GPa)	Yield stress at 0.2% offset (MPa)	Ultimate tensile stress (MPa)	Fracture stress (MPa)	Uniform elongation (%)	Total elongation (%)
Ti-6Al-4V	954	142	1010	1050	870	4.9	14.2
Ti-6Al-4V-0.020Y	954	134	950	990	835	5.0	12.5
Ti-6Al-4V-0.050Y	932	128	860	945	780	5.8	14.6
Ti-6Al-4V-0.10Y	932	135	920	980	815	5.7	12.7
Ti-6Al-4V-0.30Y	932	139	885	950	810	6.0	13.0
Ti-6Al-4V-0.010MM	932	126	905	945	800	6.8	14.4
Ti-6Al-4V-0.030MM	932	134	915	950	815	5.9	12.9
Ti-6Al-4V-0.080MM	932	147	925	970	935	6.8	14.2
Ti-6Al-4V-0.10Er	948	168	950	1010	830	5.2	14.8
Ti-6Al-4V-0.30Er	926	106	860	915	735	5.5	15.7
Ti-6Al-4V-0.80Er (Ingot 27)	926						
Ti-6Al-4V-0.80Er (Ingot 29)	926	138	880	910	755	5.6	13.6

GP77-0480-23

TABLE A3. ROOM-TEMPERATURE TENSILE PROPERTIES OF PHASE I Ti-6Al-4V-RE ALLOYS ANNEALED AT $T_\beta - 56^\circ C$ FOR 60 min

Alloy composition	Annealing temperature, $T_\beta - 56^\circ C$ (°C)	Elastic modulus (GPa)	Yield stress at 0.2% offset (MPa)	Ultimate tensile stress (MPa)	Fracture stress (MPa)	Uniform elongation (%)	Total elongation (%)
Ti-6Al-4V	954	118	950	1030	885	4.7	12.0
Ti-6Al-4V-0.020Y	954	158	885	975	950	5.9	13.8
Ti-6Al-4V-0.050Y	932	150	885	935	845	6.1	15.2
Ti-6Al-4V-0.10Y	932	135	910	1000	840	5.3	13.7
Ti-6Al-4V-0.30Y	932	124	935	965	830	6.0	13.4
Ti-6Al-4V-0.010MM	932	128	855	940	810	5.8	12.0
Ti-6Al-4V-0.030MM	932	142	890	930	780	6.2	14.1
Ti-6Al-4V-0.080MM	932	132	925	970	870	6.1	12.8
Ti-6Al-4V-0.10Er	948	154	975	1025	830	4.9	14.8
Ti-6Al-4V-0.30Er	926	102	850	900	740	4.7	13.6
Ti-6Al-4V-0.80Er (Ingot 27)	926	131	865	925	780	4.9	12.1
Ti-6Al-4V-0.80Er (Ingot 29)	926	150	890	915	780	5.4	11.7

GP77-0480-24

TABLE A4. ROOM-TEMPERATURE TENSILE PROPERTIES OF PHASE I Ti-6Al-4V-RE ALLOYS ANNEALED AT $T_\beta - 56^\circ C$ FOR 180 min

Alloy composition	Annealing temperature, $T_\beta - 56^\circ C$ (°C)	Elastic modulus (GPa)	Yield stress at 0.2% offset (MPa)	Ultimate tensile stress (MPa)	Fracture stress (MPa)	Uniform elongation (%)	Total elongation (%)
Ti-6Al-4V	954	138	970	1055	930	4.6	10.2
Ti-6Al-4V-0.020Y	954	125	920	995	855	3.9	10.4
Ti-6Al-4V-0.050Y	932	136	860	950	825	3.7	8.5
Ti-6Al-4V-0.10Y	932	125	900	975	810	4.8	13.3
Ti-6Al-4V-0.30Y	932	136	905	970	835	4.8	10.0
Ti-6Al-4V-0.010MM	932	145	875	950	825	5.4	11.0
Ti-6Al-4V-0.030MM	932	127	815	925	815	6.1	12.8
Ti-6Al-4V-0.080MM	932	133	870	955	855	6.3	13.8
Ti-6Al-4V-0.10Er	948	145	955	1005	835	4.4	13.0
Ti-6Al-4V-0.30Er	926	113	885	935	810	4.7	12.1
Ti-6Al-4V-0.80Er (Ingot 27)	926	125	840	900	765	5.1	12.6
Ti-6Al-4V-0.80Er (Ingot 29)	926	123	885	920	795	5.0	11.8

GP77-0480-25

TABLE A5. ROOM-TEMPERATURE TENSILE PROPERTIES OF PHASE I Ti-6Al-4V-RE ALLOYS ANNEALED AT $T_\beta - 28^oC$ FOR 15 min

Alloy composition	Annealing temperature, $T_\beta - 28^oC$ (°C)	Elastic modulus (GPa)	Yield stress at 0.2% offset (MPa)	Ultimate tensile stress (MPa)	Fracture stress (MPa)	Uniform elongation (%)	Total elongation (%)
Ti-6Al-4V	982	129	970	1050	915	3.7	10.0
Ti-6Al-4V-0.020Y	982	140	965	1010	835	4.3	12.1
Ti-6Al-4V-0.050Y	960	127	855	960	805	5.1	11.2
Ti-6Al-4V-0.10Y	960	126	880	965	820	5.2	12.3
Ti-6Al-4V-0.30Y	960	128	930	965	825	3.5	10.5
Ti-6Al-4V-0.010MM	960	133	870	935	815	5.7	11.7
Ti-6Al-4V-0.030MM	960	127	855	940	820	5.1	10.8
Ti-6Al-4V-0.080MM	960	133	920	970	845	5.6	13.5
Ti-6Al-4V-0.10Er	976	133	985	1030	830	4.3	12.8
Ti-6Al-4V-0.30Er	954	109	965	1020	820	4.3	12.2
Ti-6Al-4V-0.80Er (Ingot 27)	954	133	955	1005	825	4.8	12.0
Ti-6Al-4V-0.80Er (Ingot 29)	954	140	970	1015	860	3.9	10.3

GP77-0480-26

TABLE A6. ROOM-TEMPERATURE TENSILE PROPERTIES OF PHASE I Ti-6Al-4V-RE ALLOYS ANNEALED AT $T_\beta - 28^oC$ FOR 30 min

Alloy composition	Annealing temperature, $T_\beta - 28^oC$ (°C)	Elastic modulus (GPa)	Yield stress at 0.2% offset (MPa)	Ultimate tensile stress (MPa)	Fracture stress (MPa)	Uniform elongation (%)	Total elongation (%)
Ti-6Al-4V	982	126	1020	1085	930	5.1	14.9
Ti-6Al-4V-0.020Y	982	128	970	1040	925	3.7	8.3
Ti-6Al-4V-0.050Y	960	134	905	980	815	5.1	12.2
Ti-6Al-4V-0.10Y	960	147	990	1030	865	5.1	12.4
Ti-6Al-4V-0.30Y	960	142	1000	1040	900	4.9	12.3
Ti-6Al-4V-0.010MM	960	128	905	970	830	6.1	12.5
Ti-6Al-4V-0.030MM	960	140	845	950	840	6.3	12.3
Ti-6Al-4V-0.080MM	960	124	950	1000	885	5.1	11.6
Ti-6Al-4V-0.10Er	976	130	1010	1060	850	4.2	13.8
Ti-6Al-4V-0.30Er	954	108	960	1015	840	4.6	13.3
Ti-6Al-4V-0.80Er (Ingot 27)	954						
Ti-6Al-4V-0.80Er (Ingot 29)	954	140	930	980	840	4.6	11.7

GP77-0480-27

TABLE A7. ROOM-TEMPERATURE TENSILE PROPERTIES OF PHASE I Ti-6Al-4V-RE ALLOYS ANNEALED AT T_β – 28°C FOR 60 min

Alloy composition	Annealing temperature, T_β – 28°C (°C)	Elastic modulus (GPa)	Yield stress at 0.2% offset (MPa)	Ultimate tensile stress (MPa)	Fracture stress (MPa)	Uniform elongation (%)	Total elongation (%)
Ti-6Al-4V	982	131	950	1025	910	4.8	12.3
Ti-6Al-4V-0.020Y	982	142	970	1040	930	3.8	8.3
Ti-6Al-4V-0.050Y	960	138	905	995	865	5.0	11.5
Ti-6Al-4V-0.10Y	960	142	930	1015	890	5.1	13.8
Ti-6Al-4V-0.30Y	960	135	960	1045	900	4.9	12.5
Ti-6Al-4V-0.010MM	960	150	900	995	875	4.7	9.8
Ti-6Al-4V-0.030MM	960	137	920	980	830	5.8	13.3
Ti-6Al-4V-0.080MM	960	119	980	985	910	6.0	13.1
Ti-6Al-4V-0.10Er	976	147	1030	1085	865	4.1	15.2
Ti-6Al-4V-0.30Er	954	103	940	1000	825	4.6	13.4
Ti-6Al-4V-0.80Er (Ingot 27)	954	129	935	985	860	4.0	8.6
Ti-6Al-4V-0.80Er (Ingot 29)	954	142	965	1015	870	3.8	10.2

GP77-0480-28

TABLE A8. ROOM-TEMPERATURE TENSILE PROPERTIES OF PHASE I Ti-6Al-4V-RE ALLOYS ANNEALED AT T_β – 28°C FOR 180 min

Alloy composition	Annealing temperature, T_β – 28°C (°C)	Elastic modulus (GPa)	Yield stress at 0.2% offset (MPa)	Ultimate tensile stress (MPa)	Fracture stress (MPa)	Uniform elongation (%)	Total elongation (%)
Ti-6Al-4V	982	120	985	1060	970	3.8	9.2
Ti-6Al-4V-0.020Y	982	121	1005	1075	915	3.3	10.8
Ti-6Al-4V-0.050Y	960	136	930	1005	870	4.4	10.4
Ti-6Al-4V-0.10Y	960	130	920	1010	880	3.9	10.9
Ti-6Al-4V-0.30Y	960	142	1000	1060	945	4.7	11.3
Ti-6Al-4V-0.010MM	960	126	955	1020	895	4.7	10.8
Ti-6Al-4V-0.030MM	960	123	900	960	865	5.7	12.2
Ti-6Al-4V-0.080MM	960	143	915	990	890	5.4	11.9
Ti-6Al-4V-0.10Er	976	140	1020	1080	860	3.5	14.0
Ti-6Al-4V-0.30Er	954	107	985	1040			2.6
Ti-6Al-4V-0.80Er (Ingot 27)	954	139	935	995	850	3.2	9.2
Ti-6Al-4V-0.80Er (Ingot 29)	954	140	970	1020	905	4.2	11.4

GP77-0480-29

TABLE A9. ROOM-TEMPERATURE TENSILE PROPERTIES OF PHASE I Ti-6Al-4V-RE ALLOYS ANNEALED AT T_β + 28°C FOR 5 min

Alloy composition	Annealing temperature, T_β + 28°C (°C)	Elastic modulus (GPa)	Yield stress at 0.2% offset (MPa)	Ultimate tensile stress (MPa)	Fracture stress (MPa)	Uniform elongation (%)	Total elongation (%)
Ti-6Al-4V	1038	138	1045	1125	990	2.5	12.0
Ti-6Al-4V-0.020Y	1038	148	990	1060	940	3.6	10.9
Ti-6Al-4V-0.050Y	1016					3.8	10.5
Ti-6Al-4V-0.10Y	1016	148	960	1060	940	3.3	10.0
Ti-6Al-4V-0.30Y	1016	143	1010	1080	950	3.8	11.5
Ti-6Al-4V-0.010MM	1016	150	945	1030	945	3.9	9.1
Ti-6Al-4V-0.030MM	1016	141	985	1055	1000	5.0	9.5
Ti-6Al-4V-0.080MM	1016	120	1015	1070	1035	3.5	7.7
Ti-6Al-4V-0.10Er	1032	135	1015	1075	925	3.4	11.8
Ti-6Al-4V-0.30Er	1016	132	1005	1075	910	3.5	12.2
Ti-6Al-4V-0.80Er (Ingot 27)	1010						
Ti-6Al-4V-0.80Er (Ingot 29)	1010	148	980	1060	960	3.6	10.4

GP77-0480-30

TABLE A10. ROOM-TEMPERATURE TENSILE PROPERTIES OF PHASE I Ti-6Al-4V-RE ALLOYS ANNEALED AT T_β + 28°C FOR 15 min

Alloy composition	Annealing temperature, T_β + 28°C (°C)	Elastic modulus (GPa)	Yield stress at 0.2% offset (MPa)	Ultimate tensile stress (MPa)	Fracture stress (MPa)	Uniform elongation (%)	Total elongation (%)
Ti-6Al-4V	1038	150	1085	1165	1105	2.4	9.2
Ti-6Al-4V-0.020Y	1038	154	1040	1110	1000	3.4	9.9
Ti-6Al-4V-0.050Y	1016	152	1025	1085	950	3.0	9.0
Ti-6Al-4V-0.10Y	1016	124	1030	1090	980	3.9	10.4
Ti-6Al-4V-0.30Y	1016	156	1045	1105	960	3.4	9.8
Ti-6Al-4V-0.010MM	1016	144	1030	1095	1040	3.3	8.2
Ti-6Al-4V-0.030MM	1016	150	1015	1055	990	3.8	9.1
Ti-6Al-4V-0.080MM	1016	153	1005	1090	1050	3.0	6.8
Ti-6Al-4V-0.10Er	1032	138	1060	1125	1000	3.7	11.0
Ti-6Al-4V-0.30Er	1016	132	1005	1075	925	3.3	10.5
Ti-6Al-4V-0.80Er (Ingot 27)	1010	135	970	1050	910	4.3	10.8
Ti-6Al-4V-0.80Er (Ingot 29)	1010	144	1000	1070	955	3.9	10.3

GP77-0480-31

TABLE A11. ROOM-TEMPERATURE TENSILE PROPERTIES OF PHASE I Ti-6Al-4V-RE ALLOYS ANNEALED AT T_β + 28°C FOR 30 min

Alloy composition	Annealing temperature, T_β + 28°C (°C)	Elastic modulus (GPa)	Yield stress at 0.2% offset (MPa)	Ultimate tensile stress (MPa)	Fracture stress (MPa)	Uniform elongation (%)	Total elongation (%)
Ti-6Al-4V	1038	147	1085	1040	1110	2.2	7.2
Ti-6Al-4V-0.020Y	1038	128	1000	1055	945	4.5	11.1
Ti-6Al-4V-0.050Y	1016	165	980	1095	975	4.1	11.1
Ti-6Al-4V-0.10Y	1016	135	1030	1115	1005	4.3	11.3
Ti-6Al-4V-0.30Y	1016	168	1045	1120	960	3.9	11.1
Ti-6Al-4V-0.010MM	1016	134	1030	1090	990	3.2	8.3
Ti-6Al-4V-0.030MM	1016	146	1040	1090	1030	4.1	9.1
Ti-6Al-4V-0.080MM	1016	150	1035	1105	1055	4.3	9.9
Ti-6Al-4V-0.10Er	1032	132	1055	1115	995	3.5	9.6
Ti-6Al-4V-0.30Er	1016	135	1015	1105	960	3.5	12.0
Ti-6Al-4V-0.80Er (Ingot 27)	1010						
Ti-6Al-4V-0.80Er (Ingot 29)	1010	147	1010	1080	970	3.4	9.7

GP77-0480-32

TABLE A12. ROOM-TEMPERATURE TENSILE PROPERTIES OF PHASE I Ti-6Al-4V-RE ALLOYS ANNEALED AT T_β + 28°C FOR 60 min

Alloy composition	Annealing temperature, T_β + 28°C (°C)	Elastic modulus (GPa)	Yield stress at 0.2% offset (MPa)	Ultimate tensile stress (MPa)	Fracture stress (MPa)	Uniform elongation (%)	Total elongation (%)
Ti-6Al-4V	1038	138	1070	1155	1140	1.9	3.2
Ti-6Al-4V-0.020Y	1038	150	1030	1090	1000	3.0	9.2
Ti-6Al-4V-0.050Y	1016	165	990	1090	975	4.4	11.4
Ti-6Al-4V-0.10Y	1016	158	1025	1110	1010	3.3	9.2
Ti-6Al-4V-0.30Y	1016	142	1090	1145	1020	3.6	10.6
Ti-6Al-4V-0.010MM	1016	144	1020	1080	1005	2.9	7.3
Ti-6Al-4V-0.030MM	1016	136	985	1050	995	2.1	5.3
Ti-6Al-4V-0.080MM	1016	154	1050	1110	1095	4.2	9.4
Ti-6Al-4V-0.10Er	1032	134	1045	1120	1015	3.5	9.9
Ti-6Al-4V-0.30Er	1016	130	975	1040	870	3.8	11.9
Ti-6Al-4V-0.80Er (Ingot 27)	1010	165	980	1080	930	3.8	10.2
Ti-6Al-4V-0.80Er (Ingot 29)	1010	164	1000	1095	940	4.1	11.8

GP77-0480-33

TABLE A13. ROOM-TEMPERATURE TENSILE PROPERTIES OF PHASE I Ti-6Al-4V-RE ALLOYS ANNEALED AT T_β + 56°C FOR 5 min

Alloy composition	Annealing temperature, T_β + 56°C (°C)	Elastic modulus (GPa)	Yield stress at 0.2% offset (MPa)	Ultimate tensile stress (MPa)	Fracture stress (MPa)	Uniform elongation (%)	Total elongation (%)
Ti-6Al-4V	1066	130	1020	1105	990	3.8	12.1
Ti-6Al-4V-0.020Y	1066	144	1035	1090	980	4.0	10.3
Ti-6Al-4V-0.050Y	1044	154	1000	1070	930	4.5	12.3
Ti-6Al-4V-0.10Y	1044	148	1020	1090	955	3.9	12.0
Ti-6Al-4V-0.30Y	1044	148	1030	1105	965	3.4	10.2
Ti-6Al-4V-0.010MM	1044	159	970	1065	965	4.0	10.7
Ti-6Al-4V-0.030MM	1044	134	1015	1085	980	3.0	8.8
Ti-6Al-4V-0.080MM	1044	144	1020	1090	1030	3.8	8.7
Ti-6Al-4V-0.10Er	1060	149	1020	1105	970	3.7	11.2
Ti-6Al-4V-0.30Er	1044	132	955	1010	880	3.7	10.8
Ti-6Al-4V-0.80Er (Ingot 27)	1038	139	965	1055	925	4.5	10.7
Ti-6Al-4V-0.80Er (Ingot 29)	1038	158	955	1065	940	4.2	11.3

GP77-0480-34

TABLE A14. ROOM-TEMPERATURE TENSILE PROPERTIES OF PHASE I Ti-6Al-4V-RE ALLOYS ANNEALED AT T_β + 56°C FOR 15 min

Alloy composition	Annealing temperature, T_β + 56°C (°C)	Elastic modulus (GPa)	Yield stress at 0.2% offset (MPa)	Ultimate tensile stress (MPa)	Fracture stress (MPa)	Uniform elongation (%)	Total elongation (%)
Ti-6Al-4V	1066	141	1090	1170	1155	2.6	5.8
Ti-6Al-4V-0.020Y	1066	158	1015	1095	1040	3.8	9.9
Ti-6Al-4V-0.050Y	1044	138	1005	1070	940	4.1	12.1
Ti-6Al-4V-0.10Y	1044	136	1005	1070	925	3.8	13.0
Ti-6Al-4V-0.30Y	1044	150	1020	1115	970	4.3	12.5
Ti-6Al-4V-0.010MM	1044	158	1005	1075	1035	3.8	8.3
Ti-6Al-4V-0.030MM	1044	150	1025	1080	1040	4.3	9.5
Ti-6Al-4V-0.080MM	1044	141	1020	1085	1050	3.7	8.3
Ti-6Al-4V-0.10Er	1060	138	1045	1105	985	3.7	10.7
Ti-6Al-4V-0.30Er	1044	138	975	1045	895	3.5	10.6
Ti-6Al-4V-0.80Er (Ingot 27)	1038						
Ti-6Al-4V-0.80Er (Ingot 29)	1038	140	1015	1085	1035	3.7	9.2

GP77-0480-35

TABLE A15. ROOM-TEMPERATURE TENSILE PROPERTIES OF PHASE I Ti-6Al-4V-RE ALLOYS ANNEALED AT T_β + 56°C FOR 30 min

Alloy composition	Annealing temperature, T_β + 56°C (°C)	Elastic modulus (GPa)	Yield stress at 0.2% offset (MPa)	Ultimate tensile stress (MPa)	Fracture stress (MPa)	Uniform elongation (%)	Total elongation (%)
Ti-6Al-4V	1066	170	1090	1145	1120	3.2	7.8
Ti-6Al-4V-0.020Y	1066	170	1035	1105	1065	3.8	9.4
Ti-6Al-4V-0.050Y	1044	150	1045	1100	970	4.0	11.7
Ti-6Al-4V-0.10Y	1044	151	1015	1075	955	3.7	10.6
Ti-6Al-4V-0.30Y	1044	162	1050	1120	960	4.2	14.2
Ti-6Al-4V-0.010MM	1044	156	1010	1060	1020	3.3	8.0
Ti-6Al-4V-0.030MM	1044	129	1005	1070	1030	3.3	8.0
Ti-6Al-4V-0.080MM	1044	158	1020	1085	1055	3.9	8.6
Ti-6Al-4V-0.10Er	1060	142	1080	1150	1020	3.3	11.4
Ti-6Al-4V-0.30Er	1044	142	985	1070	930	3.5	10.2
Ti-6Al-4V-0.80Er (Ingot 27)	1038	146	960	1045	910	3.6	10.5
Ti-6Al-4V-0.80Er (Ingot 29)	1038	148	1030	1070	970	3.4	8.7

GP77-0480-36

TABLE A16. ROOM-TEMPERATURE TENSILE PROPERTIES OF PHASE I Ti-6Al-4V-RE ALLOYS ANNEALED AT T_β + 56°C FOR 60 min

Alloy composition	Annealing temperature, T_β + 56°C (°C)	Elastic modulus (GPa)	Yield stress at 0.2% offset (MPa)	Ultimate tensile stress (MPa)	Fracture stress (MPa)	Uniform elongation (%)	Total elongation (%)
Ti-6Al-4V	1066	128	1105	1165	1160	2.4	4.8
Ti-6Al-4V-0.020Y	1066	150	1070	1130	1015	3.6	8.4
Ti-6Al-4V-0.050Y	1044	128	975	1050	895	3.4	12.2
Ti-6Al-4V-0.10Y	1044	142	1030	1100	975	4.0	11.5
Ti-6Al-4V-0.30Y	1044	140	1035	1100	970	2.8	8.5
Ti-6Al-4V-0.010MM	1044	147	995	1075	1020	3.0	8.8
Ti-6Al-4V-0.030MM	1044	141	1025	1070	1045	3.3	6.3
Ti-6Al-4V-0.080MM	1044	142	1000	1055	1045	3.3	6.6
Ti-6Al-4V-0.10Er	1060	143	1055	1125	1095	4.2	8.6
Ti-6Al-4V-0.30Er	1044	165	1005	1095	950	3.7	12.1
Ti-6Al-4V-0.80Er (Ingot 27)	1038	147	945	1010	875	3.1	9.6
Ti-6Al-4V-0.80Er (Ingot 29)	1038	150	1040	1110	990	3.2	9.7

GP77-0480-37

TABLE A17. ROOM-TEMPERATURE TENSILE PROPERTIES OF PHASE II Ti-6Al-4V-RE ALLOYS IN THE LONGITUDINAL (L) AND TRANSVERSE (T) DIRECTIONS; HOT-ROLLED AND ANNEALED, AS RECEIVED

Alloy composition	Processing condition	Yield stress at 0.2% offset (MPa)		Ultimate tensile stress (MPa)		Uniform elongation (%)		Total elongation (%)	
		L	T	L	T	L	T	L	T
Ti-6Al-4V	A	930	998	960	1028	5.6	3.8	11.6	10.3
	B	–	923	–	975	–	2.9	–	11.1
Ti-6Al-4V-0.02Y	A	998	910	1028	975	4.8	4.5	11.8	12.6
	B	870	960	945	1005	5.5	4.5	13.5	13.5
Ti-6Al-4V-0.05Y	A	938	1005	975	1020	4.8	4.0	14.5	11.8
	B	900	923	960	1012	5.3	4.1	13.7	12.7
Ti-6Al-4V-0.10Er	A	900	960	930	1013	6.3	3.8	14.3	12.6
	B	870	930	938	997	5.5	4.0	13.0	13.4
Ti-6Al-4V-0.038Y_2O_3	A	953	990	983	1043	5.8	5.1	15.8	13.2
	B	870	953	908	998	5.1	3.8	12.2	12.8

GP78-0635-5

Processing condition: A = continuously rolled from 26 mm to 13 mm thickness from 940°C
B = continuously rolled from 26 mm to 13 mm thickness from 1025°C

TABLE A18. ROOM-TEMPERATURE TENSILE PROPERTIES OF PHASE II Ti-6Al-4V-RE ALLOYS IN THE LONGITUDINAL (L) AND TRANSVERSE (T) DIRECTIONS; RECRYSTALLIZATION ANNEALED

Alloy composition	Processing condition	Yield stress at 0.2% offset (MPa)		Ultimate tensile stress (MPa)		Uniform elongation (%)		Total elongation (%)	
		L	T	L	T	L	T	L	T
Ti-6Al-4V	A	–	848	–	894	–	8.2	–	16.3
	B	765	758	855	848	7.3	4.0	16.2	10.8
Ti-6Al-4V-0.02Y	A	780	863	855	938	5.7	8.0	12.0	16.2
	B	780	780	855	863	6.2	4.3	16.0	16.0
Ti-6Al-4V-0.05Y	A	870	855	938	930	7.2	7.2	15.4	14.1
	B	833	745	915	878	7.2	4.5	16.2	15.8
Ti-6Al-4V-0.10Er	A	758	862	833	910	6.0	7.2	15.3	14.8
	B	788	780	870	870	7.2	4.2	16.3	14.9
Ti-6Al-4V-0.038Y_2O_3	A	855	870	923	953	6.9	8.1	16.2	16.2
	B	795	780	880	870	5.9	4.0	16.1	14.4

GP78-0635-6

Processing condition: A = continuously rolled from 26 mm to 13 mm thickness from 940°C
B = continuously rolled from 26 mm to 13 mm thickness from 1025°C

TABLE A19. ROOM-TEMPERATURE TENSILE PROPERTIES OF PHASE II Ti-6Al-4V-RE ALLOYS IN THE LONGITUDINAL (L) AND TRANSVERSE (T) DIRECTIONS; BETA ANNEALED

Alloy composition	Processing condition	Yield stress at 0.2% offset (MPa)		Ultimate tensile stress (MPa)		Uniform elongation (%)		Total elongation (%)	
		L	T	L	T	L	T	L	T
Ti-6Al-4V	A	870	855	920	923	3.3	3.6	8.5	7.7
	B	840	863	923	915	3.9	3.1	10.1	9.2
Ti-6Al-4V-0.02Y	A	877	848	953	930	5.3	3.9	12.0	8.8
	B	840	848	923	930	5.1	4.5	12.6	13.3
Ti-6Al-4V-0.05Y	A	863	855	953	947	4.4	4.9	11.5	11.0
	B	840	863	930	953	5.4	5.4	14.5	13.9
Ti-6Al-4V-0.10Er	A	840	–	915	–	4.8	–	12.8	–
	B	848	863	938	945	5.3	5.1	13.5	14.2
Ti-6Al-4V-0.038Y_2O_3	A	885	855	960	945	5.4	4.3	11.0	9.3
	B	877	885	945	945	4.9	3.8	14.0	11.2

GP78-0635-7

Processing condition: A = continuously rolled from 26 mm to 13 mm thickness from 940°C
B = continuously rolled from 26 mm to 13 mm thickness from 1025°C

TABLE A20. ROOM-TEMPERATURE TENSILE PROPERTIES OF PHASE II Ti-6Al-4V-RE ALLOYS IN THE LONGITUDINAL (L) AND TRANSVERSE (T) DIRECTIONS; SOLUTION-TREATED-AND-AGED

Alloy composition	Processing condition	Yield stress at 0.2% offset (MPa)		Ultimate tensile stress (MPa)		Uniform elongation (%)		Total elongation (%)	
		L	T	L	T	L	T	L	T
Ti-6Al-4V	A	1020	1072	1110	1178	2.4	1.8	5.0	3.8
	B	1080	–	1163	–	2.4	–	4.6	–
Ti-6Al-4V-0.02Y	A	1230	–	1298	–	–	1.8	–	4.5
	B	1103	1080	1178	1170	2.8	2.4	7.2	6.8
Ti-6Al-4V-0.05Y	A	1125	–	1200	–	–	1.7	–	4.1
	B	1110	1013	1205	1133	3.8	2.9	7.9	7.1
Ti-6Al-4V-0.10Er	A	–	–	–	–	–	–	–	–
	B	–	–	–	–	–	–	–	–
Ti-6Al-4V-0.038Y_2O_3	A	1103	–	1193	–	2.7	–	5.6	–
	B	1110	1133	1193	1200	2.8	2.4	6.6	6.1

GP78-0635-8

Processing condition: A = continuously rolled from 26 mm to 13 mm thickness from 940°C
B = continuously rolled from 26 mm to 13 mm thickness from 1025°C

TABLE A21. ROOM-TEMPERATURE TENSILE PROPERTIES OF PHASE II Ti-6Al-4V-RE ALLOYS IN THE LONGITUDINAL (L) AND TRANSVERSE (T) DIRECTIONS; SOLUTION-TREATED-AND-OVERAGED

Alloy composition	Processing condition	Yield stress at 0.2% offset (MPa)		Ultimate tensile stress (MPa)		Uniform elongation (%)		Total elongation (%)	
		L	T	L	T	L	T	L	T
Ti-6Al-4V	A	–	1020	–	1088	–	2.7	–	5.8
	B	990	975	1057	1050	3.7	3.1	7.6	5.7
Ti-6Al-4V-0.02Y	A	983	1028	1073	1080	3.8	2.9	7.8	6.9
	B	998	998	1080	1073	3.5	3.2	10.2	9.0
Ti-6Al-4V-0.05Y	A	1013	990	1088	1073	3.8	2.8	10.0	7.0
	B	998	1028	1080	1088	3.8	3.6	10.7	9.5
Ti-6Al-4V-0.10Er	A	983	990	1050	1065	3.0	2.8	9.8	6.7
	B	990	975	1073	1057	3.0	3.8	8.0	10.3
Ti-6Al-4V-0.038Y_2O_3	A	998	998	1070	1080	3.2	3.0	6.8	6.2
	B	1020	998	1088	1080	4.2	3.5	9.9	7.8

GP78-0635-9

Processing condition: A = continuously rolled from 26 mm to 13 mm thickness from 940°C
B = continuously rolled from 26 mm to 13 mm thickness from 1025°C

TABLE A22. ROOM-TEMPERATURE TENSILE PROPERTIES OF PHASE II Ti-6Al-4V-RE ALLOYS IN THE LONGITUDINAL (L) AND TRANSVERSE (T) DIRECTIONS): α-β ANNEALED AND AGED

Alloy composition	Processing condition	Yield stress at 0.2% offset (MPa)		Ultimate tensile stress (MPa)		Uniform elongation (%)		Total elongation (%)	
		L	T	L	T	L	T	L	T
Ti-6Al-4V	A	825	878	923	945	5.6	7.3	14.2	16.3
	B	795	848	900	923	6.8	5.6	16.1	13.8
Ti-6Al-4V-0.02Y	A	848	885	945	945	6.6	4.9	14.8	12.1
	B	810	855	915	923	6.1	5.2	14.2	12.2
Ti-6Al-4V-0.05Y	A	885	893	975	960	7.7	5.6	16.5	14.6
	B	825	885	923	945	5.8	5.1	15.4	10.9
Ti-6Al-4V-0.10Er	A	840	848	938	923	6.7	4.7	14.4	12.7
	B	803	870	893	945	6.2	6.6	15.1	14.6
Ti-6Al-4V-0.038Y_2O_3	A	893	893	975	960	8.3	5.4	16.2	11.4
	B	775	885	900	907	4.9	4.1	13.6	11.9

GP78-0635-10

Processing condition: A = continuously rolled from 26 mm to 13 mm thickness from 940°C
B = continuously rolled from 26 mm to 13 mm thickness from 1025°C

DISTRIBUTION

	Copies
Defense Documentation Center Cameron Station Alexandria, VA 22314	12
Office of Naval Research Department of the Navy 800 N. Quincy Street Arlington, VA 22217	
Attn: Code 471	1
Code 102	1
Code 470	1
Commanding Officer Office of Naval Research Branch Office Building 114, Section D 666 Summer Street Boston, MA 02210	1
Commanding Officer Office of Naval Research Branch Office 536 South Clark Street Chicago, IL 60605	1
Office of Naval Research San Francisco Area Office One Hallidie Plaza Suite 601 San Francisco, CA 94102	1
Naval Research Laboratory Washington, D. C. 20375	
Attn: Code 6000	1
6100	1
6300	1
6400	1
2627	1
Naval Air Development Center Code 302 Warminster, PA 18964	
Attn: Mr. F. S. Williams	1
Naval Air Propulsion Test Center Trenton, NJ 08628	1
Attn: Library	1

	Copies
Naval Construction Batallion Civil Engineering Laboratory Port Hueneme, CA 93043	
Attn: Materials Division	1
Naval Electronics Laboratory San Diego, CA 92152	
Attn: Electron Materials Sciences Division	1
Naval Missile Center Materials Consultant Code 3312-1 Point Mugu, CA 92041	1
Commanding Officer Naval Surface Weapons Center White Oak Laboratory Silver Spring, MD 20910	
Attn: Library	1
David W. Taylor Naval Ship R&D Center Materials Department Annapolis, MD 21402	1
Naval Undersea Center San Diego, CA 92132	
Attn: Library	1
Naval Underwater System Center Newport, RI 02840	
Attn: Library	1
Naval Weapons Center China Lake, CA 93555	
Attn: Library	1
Naval Postgraduate School Monterey, CA 93940	
Attn: Mechanical Engineering Department	1
Naval Air Systems Command Washington, D.C. 20360	
Attn: Code 52031	1
52032	1

	Copies
Naval Sea System Command Washington, D.C. 20362 Attn: Code 035	1
Naval Facilities Engineering Command Alexandria, VA 22331 Attn: Code 03	1
Scientific Advisor Commandant of the Marine Corps Washington, D.C. 20380 Attn: Code AX	1
Naval Ship Engineering Center Department of the Navy Washington, D.C. 20360 Attn: Code 6101	1
Army Research Office P.O. Box 12211 Triangle Park, NC 27709 Attn: Metallurgy & Ceramics Program	1
Army Materials and Mechanics Research Center Watertown, MA 02172 Attn: Research Programs Office	1
Air Force Office of Scientific Research Bldg. 410 Bolling Air Force Base Washington, D.C. 20332 Attn: Chemical Science Directorate	1
Electronics & Solid State Sciences Directorate	1
Air Force Materials Laboratory Wright-Patterson AFB Dayton, OH 45433	1
Library Building 50, Rm 134 Lawrence Radiation Laboratory Berkeley, CA	1

	Copies
NASA Headquarters Washington, D.C. 20546 Attn: Code RRM	1
NASA Lewis Research Center 21000 Brookpark Road Cleveland, OH 44135 Attn: Library	1
National Bureau of Standards Washington, D.C. 20234 Attn: Metallurgy Division	1
Inorganic Materials Div.	1
Director Applied Physics Laboratory University of Washington 1013 Northeast Forthieth Street Seattle, WA 98105	1
Defense Metals and Ceramics Information Center Battelle Memorial Institute 505 King Avenue Columbus, OH 43201	1
Metals and Ceramics Division Oak Ridge National Laboratory P.O. Box X Oak Ridge, TN 37380	1
Los Alamos Scientific Laboratory P.O. Box 1663 Los Alamos, NM 87544 Attn: Report Librarian	1
Argonne National Laboratory Metallurgy Division P.O. Box 229 Lemont, IL 60439	1
Brookhaven National Laboratory Technical Information Division Upton, Long Island New York 11973 Attn: Research Library	1
Office Of Naval Research Branch Office 1030 East Green Street Pasadena, CA 91106	1

	Copies
Professor J. W. Morris, Jr. University of California College of Engineering Berkeley, CA 94720	1
Dr. Neil E. Paton Rockwell International Science Center 1049 Camino Dos Rios P.O. Box 1085 Thousand Oaks, CA 91360	1
Mr. A. Pollack Naval Ships R&D Center Code 2821 Annapolsi, MD 21402	1
Professor W. F. Savage Rensselaer Polytechnic Institute School of Engineering Troy, New York 02181	1
Professor O. D. Sherby Stanford University Materials Sciences Division Stanford, CA 94300	1
Dr. G. Ecer Westinghouse Electric Corporation Research & Development Center Pittsburgh, PA 15235	1
Dr. E. A. Starke, Jr. Georgia Institute of Technology School of Chemical Engineering Atlanta, GA 30332	1
Professor David Turnbull Harvard University Division Engineering and Applied Physics Cambridge, MA 02138	1
Dr. F. E. Wawner University of Virginia School of Engineering and Applied Science Charlottesville, VA 22901	1
Dr. C. R. Whitsett McDonnell Douglas Research McDonnell Douglas Corporation Saint Louis, MO 63166	1
Dr. J. C. Williams Carnegie-Mellon University Department of Metallurgy and Materials Sciences Schenley Park Pittsburgh, PA 15213	1
Professor H. G. F. Wilsdorf University of Virginia School of Engineering and Applied Sciences Charlottesville, VA 22903	1
Professor R. Mehrabian University of Illinois at Urbana-Champaign 144 Mechanical Engineering Building Urbana, IL 61801	1
Dr. N. J. Grant Massachusetts Institute of Technology Department of Materials Science and Engineering Cambridge, MA 02139	1
Professor P. R. Strutt University of Connecticut School of Engineering Department of Metallurgy Storrs, CT 06268	1
Mr. I. Caplan David W. Taylor Naval Ship Research and Development Center Code 2813 Annapolis, MD 21402	1
Dr. G. R. Leverant Southwest Research Institute 3500 Culebra Road P.O. Box 28610 San Antonio, TX 78284	1

	Copies
Professor G. S. Ansell Rensselaer Polytechnic Institute Dept. of Metallurgical Engineering Troy, New York 02181	1
Professor H. K. Birnbaum University of Illinois Department of Metallurgy Urbana, IL 61801	1
Dr. E. M. Breinan United Technology Corporation United Technology Research Laboratories East Hartford, CT 06108	1
Professor H. D. Brody University of Pittsburgh School of Engineering Pittsburgh, PA 15213	1
Mr. R. Morante General Dynamics Electric Boat Division Eastern Point Road Groton, CT 06340	1
Professor J. B. Cohen Northwestern University Dept. of Material Sciences Evanston, IL 60201	1
Professor M. Cohen Massachusetts Institute of Technology Department of Metallurgy Cambridge, MA 02139	1
Professor Thomas W. Eagar Massachusetts Institute of Technology Department of Materials Science and Engineering Cambridge, MA 02139	1
Professor B. C. Giessen Northwestern University Department of Chemistry Boston, MA 02115	1
Professor D. G. Howden Ohio State University Dept. of Welding Engineering 190 West 19th Avenue Columbus, OH 43210	1
Dr. C. S. Kortovich TRW, Inc. 23555 Euclid Avenue Cleveland, OH 44117	1
Professor D. A. Koss Michigan Technological University College of Metallurgical Engineering Houghton, MI 49931	1
Professor A. Lawley Drexel University Dept. of Metallurgical Engineering Philadelphia, PA 19104	1
Professor Harris Marcus The University of Texas at Austin College of Engineering Austin, TX 78712	1
Dr. H. Margolin Polytechnic Institute of New York 333 Jay Street Brooklyn, N.Y. 11201	1
Professor K. Masubuchi Massachusetts Institute of Technology Department of Ocean Engineering Cambridge, MA 02139	1